nature communications

Article

https://doi.org/10.1038/s41467-025-60991-z

Colistin enhances caspofungin antifungal efficacy against *Aspergillus fumigatus* by modulating calcium homeostasis and stress responses

Received: 24 September 2024

Accepted: 9 June 2025

Published online: 01 July 2025

Check for updates

Laura Cristina García Carnero[1,9], Xingyue Li[2,9], Patrícia Alves de Castro[1], Camila Figueiredo Pinzan[1], Jonatas Erick Maimoni Campanella[3], Iran Malavazi[3,4], Mami Yoshimura[5], Luis Alberto Vega Isuhuaylas[6], Yoko Yashiroda[5], Charles Boone[5,6,7], Nir Osherov[8], Sara Fallah[6], Taylor Davie[6], Nicole Robbins[6], Leah Cowen[6], Ling Lu[2] ✉, Thaila Fernanda dos Reis[1,4] ✉ & Gustavo H. Goldman[1,4] ✉

Fungal infections cause more than 2.5 million deaths a year. Due to emerging antifungal drug resistance, novel strategies are urgently needed to combat life-threatening fungal diseases. Here, by screening a collection of 5297 compounds derived from three chemical libraries, we demonstrate that the antibacterial agent colistin (COL) can potentiate the fungistatic echinocandins caspofungin (CAS) and anidulafungin, as well as the structurally distinct cell wall targeting antifungal ibrexafungerp against *Aspergillus fumigatus*. Chemical and genetic screenings revealed that protein kinase C and the transcription factor SltA are involved in the mechanism of action of COL. SltA is essential for coping with calcium-limiting conditions, and the addition of calcium rescues COL-susceptibility. COL + CAS decreases *A. fumigatus* infection in human pulmonary cells, *Galleria mellonella*, and *Caenorhabditis elegans*. In summary, we demonstrate that the mechanism of COL as a synergizer of CAS against *A. fumigatus* is the disruption of the cell membrane permeability and calcium homeostasis.

Human fungal pathogens affect more than 1 billion people and cause around 6.5 million invasive fungal infections, leading to 3.8 million deaths per year, of which about 2.5 million are directly related to the fungal infections[1–3]. Despite the important health threat posed by fungi, they are often neglected and underestimated. Some of the infections caused by these fungi are superficial, but many are invasive or disseminated, which are difficult to prevent, diagnose, and treat[2]. One of these fungi is *Aspergillus fumigatus*, a filamentous saprophytic fungus that causes a wide array of clinical ailments ranging from allergic reactions to lethal disseminated infections in humans and animals[4].

[1]Faculdade de Ciências Farmacêuticas de Ribeirão Preto, Universidade de São Paulo, Ribeirão Preto, Brazil. [2]Department of Clinical Laboratory, Nanjing Drum Tower Hospital, College of Life Science, Nanjing Normal University, Nanjing, Jiangsu, China. [3]Departamento de Genética e Evolução, Centro de Ciências Biológicas e da Saúde, Universidade Federal de São Carlos, São Carlos, São Paulo, Brazil. [4]National Institute of Science and Technology in Human Pathogenic Fungi, São Paulo, Brazil. [5]RIKEN Center for Sustainable Resource Science, Wako, Saitama, Japan. [6]Department of Molecular Genetics, University of Toronto, Toronto, ON, Canada. [7]Donnelly Centre for Cellular and Biomolecular Research, University of Toronto, Toronto, ON, Canada. [8]Department of Clinical Microbiology and Immunology, Sackler School of Medicine, Tel-Aviv University, Tel-Aviv, Israel. [9]These authors contributed equally: Laura Cristina García Carnero, Xingyue Li. ✉e-mail: linglu@njnu.edu.cn; thailaf@hotmail.com; ggoldman@usp.br

A. fumigatus is an opportunistic fungus responsible for severe invasive infections in immunocompromised patients, affecting mainly the respiratory tract and causing invasive pulmonary aspergillosis (IPA), an infection with a high mortality rate[5]. Invasive aspergillosis, when diagnosed early, can have a favorable outcome, but its diagnosis is complex[6], and its treatment is difficult due to an increase of resistance in environmental and clinical strains to the already scarce available antifungal arsenal[7]. Azoles, such as voriconazole (VOR), itraconazole (ITR), isavuconazole (ISA), and posaconazole (POS), are fungicidal drugs and the first line treatment for aspergillosis, targeting the lanosterol-14-α-demethylase Cyp51A enzyme in the ergosterol synthesis pathway[8]. An increase in resistance to these drugs has been widely reported, mainly due to two mechanisms: (i) the increased expression of Cyp51 due to tandem repeat (TR) insertions into the *cyp51A* promoter region[8–11], and (ii) by point mutations in the *cyp51* coding region resulting in amino acid substitutions in the drug binding pocket[10,12–17].

Polyenes, such as amphotericin B (AMB), and echinocandins, that include caspofungin (CAS), micafungin (MICA), and anidulafungin (ANID), can be used as salvage therapy against azole-resistant strains[10,18], but with several disadvantages. For example, resistance to CAS, a fungistatic drug that noncompetitively inhibits the β−1,3-glucan synthase Fks1 affecting fungal cell wall composition and organization[19], has also been reported. This is through both Fks1-dependent and -independent mechanisms[20]. Echinocandin resistance most readily occurs through non-synonymous mutations in the *fks1* gene that affect drug binding and activity[7]. Resistance has also been reported through increases in mitochondrial reactive oxygen species (ROS) production that leads to alterations in the lipid composition of the cell membrane, which also alters the drug-enzyme interaction, leading to drug resistance[20]. A recent addition to the antifungal repertoire is the triterpenoid, fungistatic ibrexafungerp (IBX), a semi-synthetic derivative of enfumafungin[21,22]. IBX binds to the 1,3-β-D-glucan synthase, the same target of echinocandins, but is structurally-distinct and has oral bioavailability[21,22]. Ibrexafungerp's binding site is hypothesized to be partially divergent from that of the echinocandins, allowing it to maintain activity against some echinocandin-resistant isolates. On the other hand, AMB binds to the cell membrane acting as a fungicidal "sterol sponge" by forming extramembranous aggregates that extract ergosterol from lipid bilayers at the cell membrane, causing cell membrane depolarization and leakage[23]. However, this antifungal agent is highly hepatotoxic for the host, which limits its use to severe cases in which the other treatments have failed[24,25].

Thus, due to the increase in azole-resistant strains coupled with the limited number of antifungals available or in development, other strategies have been suggested to find new treatments for infections caused by fungal pathogens. One of these approaches is drug repurposing, which is the use of drugs already approved to treat other diseases, as antifungal agents by themselves or in combination with other bioactives[26,27]. Several drugs have been reported to be effective in the treatment of infectious diseases, such as the case of miltefosine (an antineoplasic agent) for the treatment of leishmaniasis[28,29], which has also been proposed as an alternative treatment for infections caused by the emerging fungal pathogen *Candida auris*[30,31]. In addition, some of these repurposing drugs have been identified as potentiators of currently used antifungals[32–36].

In this work, we screened three chemical libraries, Pharmakon, MedChem Express (MCE), and LifeArc, representing a total of 5297 compounds, searching for candidates that enhance the in vitro and in vivo activity of CAS against *A. fumigatus*. We found four compounds that do not show antifungal activity by themselves but that inhibit *A. fumigatus* growth in combination with CAS: lercanidipine (LER), aprotinin, cyclic somatostatin, and colistin sulfate (COL; also known as polymyxin E). Among these compounds, we decided to focus on COL. We show that COL converts CAS, a fungistatic drug, into a fungicidal drug and affects calcium availability to *A. fumigatus*. Although the use of COL in combination with azoles and echinocandins has already been reported to have a synergistic effect against clinical isolates of human pathogenic fungi like *Candida* spp, *Cryptococcus neoformans*, *A. flavus*, *A. fumigatus*, *A. terreus*, *A. nidulans*, and *A. niger*[37–46], its mode of action (MoA) has hardly been explored. Here, we demonstrate that COL disrupts calcium homeostasis in *A. fumigatus* by calcium deprivation. We identified the protein kinase C (PkcA) and the transcription factor SltA as the major determinants of COL susceptibility. Overall, we demonstrate the potential of COL as a novel antifungal strategy to synergize with fungistatic drugs converting them to fungicidal combinations against *A. fumigatus*.

Results

Identification of compounds that potentiate CAS

To identify compounds that can enhance or synergize with CAS activity against *A. fumigatus*, we used the Minimal Effective Concentration (MEC) assay to screen the fungus susceptibility to three chemical drug libraries (1600 compounds from Pharmakon library, http://www.msdiscovery.com/pharmakon.html; 2592 compounds from the MCE library, https://www.medchemexpress.com/; and 1105 compounds from LifeArc, https://www.lifearc.org/), totaling 5297 compounds. The main rationale of this screening was to identify compounds that can potentiate CAS and eventually transform this fungistatic drug into a fungicidal drug, i.e., the conidia will not able to germinate when exposed to the presence of a potentiator and CAS. Four hits, lercanidipine (LER), aprotinin, cyclic somatostatin, and colistin (COL), were identified, inhibiting 40 to 80% of the metabolic activity only in the presence of the echinocandin (Fig. 1a). LER is a calcium channel blocker (Fig. 1b) and it is used to treat hypertension[47]. Aprotinin is a protease inhibitor commonly used against viral respiratory diseases[48]. Cyclic somatostatin binds to G-protein coupled receptors (GPCRs), decreasing intracellular cyclic AMP and calcium while simultaneously increasing outward potassium currents[49]. COL is a cationic peptide antibiotic (Fig. 1c) used as the last resort antibiotic to treat infections caused by multidrug-resistant Gram-negative bacteria such as *Acinetobacter baumannii*[50]. COL binds with anionic lipopolysaccharide (LPS) molecules by displacing Mg^{2+} and Ca^{2+} from the outer cell membrane of Gram-negative bacteria, leading to permeability changes in the cell envelope and leakage of cell contents[51]. We decided to start our analysis by investigating the MoA of LER and COL due to their easy availability. The minimal inhibitory concentrations for LER and COL are >250 and >160 μM, respectively. When combined with CAS, concentrations as low as 10 μM of COL and 3.95 μg/mL LER showed a 100% fungicidal effect as determined by culturing *A. fumigatus* with compound combinations for 48 h and plating for colony forming units (CFUs) on compound-free medium (Fig. 1d, e). Thus, high-throughput screening of drug-repurposing libraries identified LER and COL as strong echinocandin potentiators with fungicidal effects.

COL enhances membrane permeability and damages mitochondria in *A. fumigatus*

To determine if the antifungal activity of LER and COL were only enhanced in the presence of CAS or whether potentiation occurred with other antifungals, we performed dose-response matrix or checkerboard assays with our hit compounds in combination with the echinocandin anidulafungin (ANID), the triterpenoid IBX, or the azole VOR. We used the SynergyFinder2.0 (https://synergyfinder.fimm.fi)[52] to calculate the interaction score between the compounds. The interaction between the drugs was classified based on the synergy score where values lower than −10 were considered antagonistic, values from −10 to 10 were considered additive and values higher than 10 were considered synergistic. Checkerboard assays showed that LER + CAS and and LER + IBX had synergistic interactions (Synergy

https://doi.org/10.1038/s41467-025-60991-z

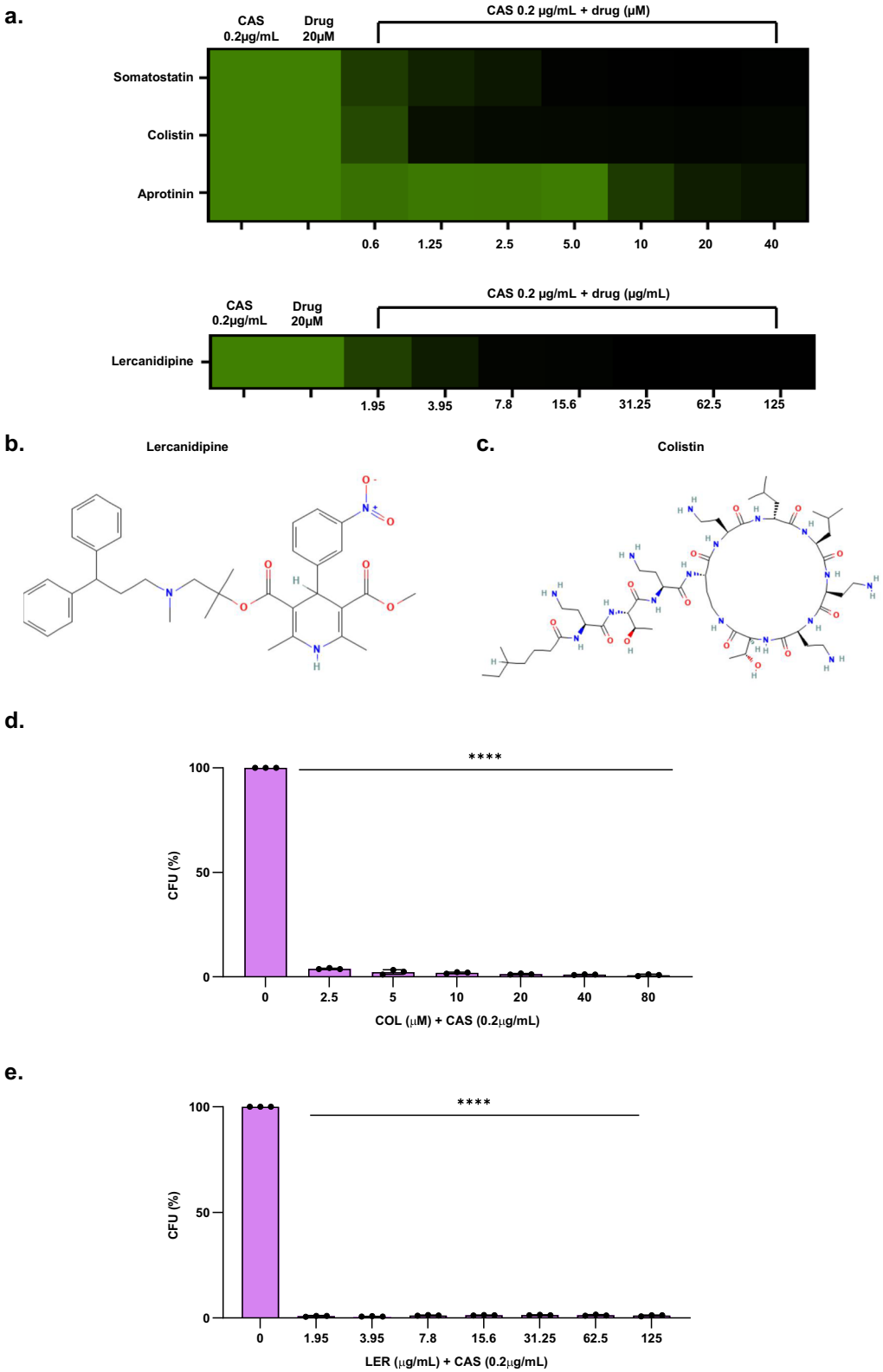

Fig. 1 | LER and COL potentiate CAS against *A. fumigatus*. **a** Metabolic activity (%) of *A. fumigatus* with the four compounds identified as potentiators of CAS activity. *A. fumigatus* was grown in liquid minimal medium (MM) with 10% of Alamar blue using 96-well plates at 37 °C in the presence of different concentrations of each drug combined with 0.2 µg/mL of CAS. After 48 h, the metabolic activity (%) was assessed by reading fluorescence at a wavelength of 570 nm excitation/590 nm emission. The results represent the average of two independent experiments performed in technical duplicate. **b**, **c** Structures of Lercanidipine (LER) and Colistin (COL). **d**, **e** Fungicidal activities of COL + CAS and LER + CAS against *A. fumigatus*. Conidia (1×10^4/mL) were incubated with 0.2 µg/mL of CAS and different concentrations of LER and COL in 96-well plates. After 48 h at 37 °C, the plates were centrifuged, the supernatants with the drugs were removed, and the cells were plated on solid MM and incubated for 48 h at 37 °C. The results represent the average of three independent experiments ± standard deviation (SD). The data was statistically analyzed by the ordinary one-way ANOVA and Dunnett´s post-test ($n = 3$; $^{*}p < 0.0001$). Source data are provided as a Source Data file.

scores of 17.289 and 26.90, respectively: Fig. 2a) while LER + ANID displayed no interactions (Synergy score of 8.19; Fig. 2b, c). COL + CAS, COL + ANID, and COL + IBX had synergistic interactions against *A. fumigatus* (Synergy scores of 28.57, 29.50, and 38.08, respectively; Fig. 2e–g). These results indicate that COL and LER can synergistically potentiate cell wall targeting CAS and IBX. Next, we wanted to determine whether COL and LER could enhance the efficacy of other antifungals with different MoA or whether they were specific to cell wall targeting compounds. We performed checkerboards with the azole VOR and observed no compound interaction with LER or COL (Synergy score of 4.54 and 0.902, respectively) (Fig. 2d, h).

We decided to concentrate our further studies on COL due to its importance as an antibacterial agent[50]. We evaluated if the combination of COL + CAS could inhibit CAS-resistant *A. fumigatus* strains (Table 1). Specifically, we tested a range of concentrations up to 80 μM COL combined with 0.25–4 μg/mL CAS. COL had no activity against three CAS-resistant clinical strains with known *fks1* mutations [MEC CAS of 16 μg/mL; strains DPL1033, MD24053 (both strains hold a S679P substitution), and EMRFP-S678P (that holds a S678P substitution[53];). COL + CAS combinations did not inhibit the growth of all tested strains (Table 1). We also tested if COL + IBX could inhibit the growth of these CAS-resistant strains (Table 1). COL clearly potentiated IBX activity against CAS-resistant strains of *A. fumigatus* (Table 1). Aiming to determine if COL + CAS-resistant strains readily emerge in *A. fumigatus*, the A1163 strain was assayed for mutation rates by using a modified Luria-Delbruck fluctuation test[54,55], using 8 μg/mL VOR as a control. Replicate cultures grown without selection were challenged on MM containing VOR or COL + CAS to determine the probability that cells would spontaneously gain mutations that provide VOR or COL + CAS resistance. In the presence of VOR, we observed a spontaneous mutation rate of 3.0×10^{-10} (95% confidence interval), while no COL + CAS-resistant mutants were observed on the MM containing COL + CAS.

This additional experiment highlights the concomitant usage of COL + CAS prevents the CAS-resistance acquisition as determined by Luria-Delbruck fluctuation tests and suggests IBX + CAS is an effective therapeutic strategy for treating CAS-resistant *A. fumigatus* infections.

Since COL impacts bacterial cell permeability, we decided to verify if there is any interaction between COL and agents that affect the cell membrane composition and, consequently, its permeability. Checkerboard assays with COL and cerulenin (CER), a molecule that inhibits fatty acid and steroid biosynthesis[56], and COL and myriocin (MYR), an inhibitor of the first step in glycosphingosine biosynthesis[57,58], showed no interactions (synergy score: 6.79) and antagonist interactions (synergy score: -11.04), respectively (Supplementary Fig. 1a and 1b). The antagonism observed led us to hypothesize that COL may be affecting sphingolipid biosynthesis and/or cell membrane organization and architecture, leading to increased membrane permeability and cell death when combined with CAS. Therefore, we tested cell viability using propidium iodide (PI), a fluorescent DNA-binding dye that freely penetrates cell membranes of dead or dying cells but is excluded from viable cells. When *A. fumigatus* germlings were incubated with 10 μM COL from 5 to 30 min, 20 to 25% of the germlings were PI^+ (Fig. 3a), while 0.03 μg/mL CAS and the combination of COL with CAS yielded 20–60% and 80–95% PI^+, respectively (Fig. 3a).

Mitochondria are the major site of ATP production. Fungal mitochondria without any stress are seen enriched as tubular and dynamic networks, but in the presence of antifungals or other stresses, the mitochondria begin to fragment, which is an indicator of cellular death[59–61] (see a representative image in Fig. 3b). We constructed an *A. fumigatus* strain whose the mitochondria constitutively express GFP. We grow this strain 16 h at 37 °C in MM then exposed (or not) the germlings to COL, CAS or the combination of this drugs and counted the germlings that had fragmented mitochondria. About 15% mitochondrial fragmentation was observed when *A. fumigatus* was grown in the absence of any drug (control minimal medium, MM) (Fig. 3b). However, when germlings were treated with COL (10 μM), CAS (0.03 μg/mL), or a combination of COL + CAS, 20%, 35%, and 90% of the germlings showed mitochondrial fragmentation (Fig. 3b). In addition, we subjected cellular extracts from wild-type strain previously grown for 24 h at 37 °C and exposed to control treatment, COL (40 μM), CAS (0.5 μg/mL) or the combination for additional 4 h at the same temperature. Higher drug concentrations were used than the experiments with germlings because mycelia are in general more resistant to drugs. Mitochondrial function was evaluated by their respiratory competence by measuring the total ATP production (Fig. 3d). When compared with the control, there was a reduction of about 25% total ATP upon exposure to COL or CAS and 60% upon exposure to a combination of COL + CAS (Fig. 3d). The decrease in the total ATP production of COL + CAS-treated wild-type cells is in agreement with the observed organellar fragmentation. Collectively, these results suggest that the COL + CAS combination causes cell death of *A. fumigatus* by increasing the cell permeability and damaging the mitochondria.

It is already known that the activation of fungal metacaspases, for example during oxidative stress, induces markers of apoptosis-like cell death such as nuclear condensation, disorganization of the histone complex, and DNA double-strand breaks, which coincide with the loss of fungal cell viability[60]. A fluorescent histone 2 A construct (h2A::mRFP) has been used as a marker of cell death in *A. fumigatus*[62]. To check if the COL + CAS compound combination induced apoptosis-like cell death, germlings of the *A. fumigatus* h2A::mRFP strain were exposed to H_2O_2 (10 mM), COL (10 or 20 μM), CAS (0.03 or 0.2 μg/mL), or CAS with COL for 1 h. The nuclei were stained with Hoechst. The H_2O_2 positive control showed complete loss of red fluorescence, indicative of a disorganized histone complex (a representative image is shown in Fig. 3c). However, no differences in mRFP fluorescence were observed in the germlings exposed to either COL, CAS, or the combination of both (Fig. 3c). This suggests COL and CAS do not induce apoptosis-like cell death.

Chemogenomic profiling in *S. cerevisiae* suggests COL impacts stress-responsive kinase

While our preliminary characterization of COL suggests that it enhances cellular permeability, the mechanism by which it does so remained elusive. As an additional tool to investigate COL MoA, we performed several screens using haploid deletion (ScWG), temperature-sensitive (TS), overexpression (MoBY), and heterozygous deletion (HET, haploinsufficiency profiling) strain libraries of the model yeast *Saccharomyces cerevisiae*[63,64]. Pooled cultures of barcoded *S. cerevisiae* strains from these collections were grown in liquid YPGal medium for 24 h at 26 °C (for TS library) or 30 °C (for the other libraries). The relative abundance of each barcoded strain following COL treatment was then determined by high throughput sequencing of PCR-amplified barcodes followed by BEAN-counter analysis[65] to measure enrichment or depletion of each strain in the presence of COL relative to solvent control (Supplementary Datas 1 to 4). For all these analyses, we considered strains as enriched or depleted when log2 fold values of ≥2 or ≤ −2 were determined, respectively.

Of 3642 genes from the *S. cerevisiae* haploid deletion library (ScWG), the normalized log read count profile showed 394 mutants that were depleted and 263 that were enriched when grown in the presence of COL (30 μM to 50 μM corresponding to 45.7% to 76.7% reduction in growth when compared to no compound controls) (Supplementary Data 1). The haploid deletion library signature of COL featured significant depletion of many mutants for genes associated with the ATG1 autophagy signaling complex, piecemeal microautophagy of nucleus, actin cytoskeleton organization, CVT pathway, macroautophagy, and transport (Supplementary Data 1). Among the top 20 mutants depleted

https://doi.org/10.1038/s41467-025-60991-z

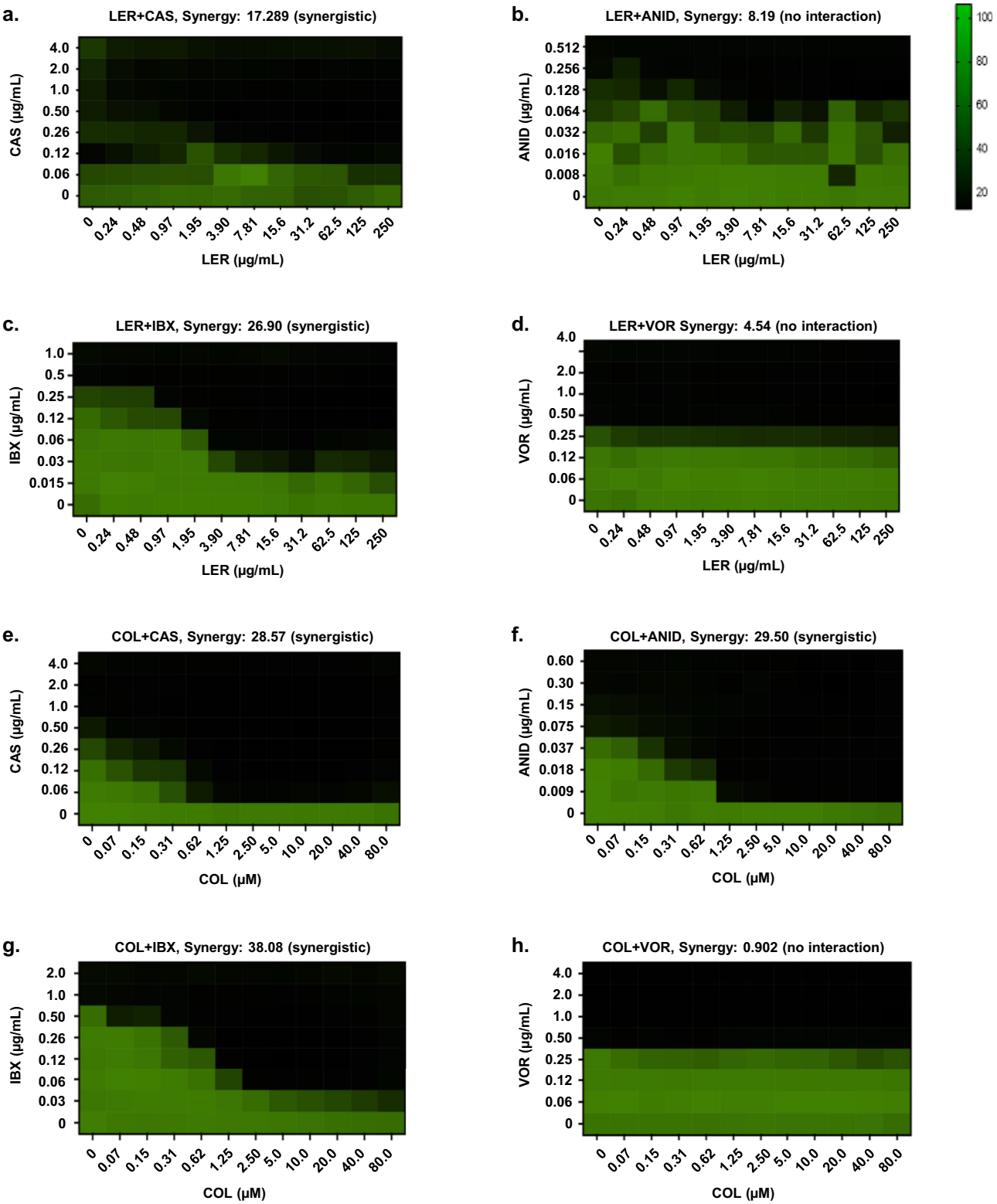

Fig. 2 | Metabolic activity assays after exposure of *A. fumigatus* to COL or LER in combination with CAS, ANID, IBX, and VOR. The synergy scores for LER x CAS (**a**), LER x ANID (**b**), LER x IBX (**c**), LER x VOR (**d**), COL x CAS (**e**), COL x ANID (**f**), COL x IBX (**g**), and COL x VOR (**h**) were determined by the analysis of the checkerboard data using the SynergyFinder software. *A. fumigatus* was grown in liquid MM using 96-well plates at 37 °C in the presence of different concentrations of the selected drugs, and after 48 h the % of metabolic activity was assessed with Alamar blue by reading fluorescence at a wavelength of 570 nm excitation/590 nm emission. A synergy score less than −10 suggests an antagonistic interaction, from −10 to 10 suggests no interaction, and larger than 10 suggests a synergistic interaction. The results represent the average of two independent experiments (Supplementary Data 9). Source data are provided as a Source Data file.

Table 1 | Synergistic combinations of COL, CAS, and IBX against *A. fumigatus* strains

Strains	CAS MEC (μg/mL)	IBX MEC (μg/mL)	COL MIC (μM)	COL (μM) + CAS (μg/mL)	COL (μM) + IBX (μg/mL)
A1163	0.25	1.0	>80	0.31 + 0.25	0.31 + 0.25
DPL1033	16	1.0	>80	>(80 + 4)	20 + 0.5
MD24053	16	1.0	>80	>(80 + 4)	20 + 0.5
EMFR-S678P	16	1.0	>80	>(80 + 4)	20 + 0.5

(strains hypersensitive to the compound), we observed enrichment for genes encoding proteins important for cation homeostasis such as: (i) the multidrug resistance Pdr5p that pumps cations and small molecules out of the cytoplasm; (ii) Hal5p, a Snf1p-related nutrient-responsive protein kinase whose overexpression increases sodium and lithium tolerance, whereas gene disruption increases cation sensitivity; and (iii) Sat4p, a protein kinase involved in salt tolerance (Supplementary Fig. 2a and Supplementary Data 1). We also identified genes encoding proteins involved in ergosterol and inositol metabolism, such as: (i) Ipt1p, an inositolphosphotransferase; and (ii) Kes1p, a sterol/phosphatidylinositol-4-phosphate (PI(4)P) exchanger (Supplementary Fig. 2a and Supplementary Data 1).

In the HET analysis, there were 56 mutants depleted and 29 mutants enriched in the presence of COL (30 μM to 50 μM corresponding to 46.7% to 74.7% reduction in growth when compared to no compound controls) (Supplementary Data 2). The HET library signature of COL featured significant depletion of many mutants for genes associated with chromatin modification and remodeling, and DNA replication and transcription (Supplementary Data 2). Among the top 20 mutants depleted, we observed enrichment for genes encoding proteins such as: (i) Neo1p, a phospholipid translocase (flippase) that plays an important role in phospholipid asymmetry of plasma membrane; (ii) Cmd1p, calmodulin, which is essential for calcium metabolism; and (iii) Tip20p, a peripheral membrane protein required for COPI vesicle fusion to the ER (Supplementary Fig. 2b and Supplementary Data 2).

In the overexpression library (MoBY), we identified 67 strains that were depleted in the presence of COL (50 to 70 μM leading to 14.4% to 44.8% reduction in growth when compared to no compound controls) (Supplementary Data 3). The MoBY library signature of COL featured significant depletion of many mutants for genes once more associated with chromatin modification and remodeling, and DNA replication and transcription (Supplementary Data 3). Among the top 20 mutants depleted, we observed enrichment for genes encoding proteins involved in ergosterol and lipid metabolism, endocytosis and secretion such as: (i) Erg1p, squalene epoxidase, essential for ergosterol biosynthesis; (ii) Sec14p, phosphatidylinositol/phosphatidylcholine transfer protein, involved in regulating phosphatidylinositol, phosphatidylcholine, and ceramide metabolism; (iii) Sec62p, essential subunit of Sec63 complex, important for protein targeting and import into the endoplasmic reticulum; and (iv) Ypt1, Rab family GTPase, involved in the ER-to-Golgi step of the secretory pathway (Supplementary Fig. 2c and Supplementary Data 3).

In the temperature-sensitive (TS) library, we identified 63 strains that were depleted in the presence of COL (10 to 30 μM corresponding to 47.1% 91.9% reduction in growth when compared to no compound controls) (Supplementary Data 4). The TS library signature of COL featured significant depletion of many mutants for genes associated with iron homeostasis and regulation of mitotic metaphase/anaphase transition (Supplementary Data 4). Among the top 20 mutants depleted, we observed enrichment for genes encoding: (i) Neo1p, a phospholipid translocase that plays a role in phospholipid asymmetry of plasma membrane; (ii) Tap42p, an essential protein involved in the TOR signaling pathway; and (iii) Cdc10p, a component of the septin ring, required for cytokinesis.

We also examined combinations of antifungal compounds. We used the SynergyFinder2.0 (https://synergyfinder.fimm.fi)[52] to calculate the interaction score between COL and the other antifungal compounds, as described above. COL potentiated fluconazole (FLUCO) and CAS with cidal effects against *S. cerevisiae*, with synergistic scores of 19.17 and 18.98, respectively (Supplementary Fig. 2e).

Taken together, these results suggest that the MoA of COL in *S. cerevisiae* involves genes involved in diverse cellular processes, including those related to autophagy, chromatin remodeling, iron homeostasis, cell permeability, protein kinases involved in salt tolerance homeostasis, protein kinase C and the cell wall integrity pathway, casein kinases, and calcium metabolism.

Impairment of *pkcA* enhances COL efficacy

Taking into consideration that the chemogenomic screening with *S. cerevisiae* provided information about the involvement of kinases in the COL MoA, we decided to screen 111 *A. fumigatus* mutants with deletion of genes encoding catalytic subunits of diverse non-essential protein kinases[66]. Culture of the mutants in the presence of 20, 40, and 80 μM COL, or 0.3 or 0.6uM COL combined with 0.2 μg/mL CAS, did not reveal any mutants more susceptible to COL relative to the corresponding wild-type strain. To further assess the COL MoA, a collection of 58 protein kinase inhibitors (PKI, at a concentration of 20 μM; Supplementary Data 5) was screened for effects on *A. fumigatus* growth, and corresponding metabolic activity alone or together with COL (2.5 μM) was measured using an XTT metabolic assay. Only one PKI, enzaustarin, a protein kinase C inhibitor that binds to the catalytic domain of mammalian PKCβ[67], potentiated COL activity against *A. fumigatus* with some single agent activity observed at high concentrations (Fig. 4a). To further confirm these results, we used an additional inhibitor of the PKC, calphostin C, that interacts with the regulatory domain of the PkcA[68], in the presence or absence of COL (20 μM). The metabolic activity of *A. fumigatus* decreased with the combination of calphostin C with COL, starting at a concentration of 25 μg/mL of the PKI (Fig. 4b).

A. fumigatus pkcA is an essential gene important for the activation of the CWI through the mitogen-activated protein kinase (MAPK) MpkA[69]. The transcription factor RlmA is important for the CWI pathway activation and it is positioned downstream of the PkcA and MpkA[70]. We constructed a conditional *pkcA* mutant by replacing the *pkcA* endogenous promoter by the inducible *xylP* promoter from *Penicillium chrysogenum*, which is induced by xylose and repressed by glucose[71]. The *xylP::pkcA* strain is unable to grow in the presence of 1% glucose but it can grow when 1% xylose is added to the medium as the sole carbon source (Fig. 4c). When wild-type and *xylP::pkcA* strains were grown in minimal medium supplemented with carbon source rations, the *xylP::pkcA* strain was more susceptible to COL with decreasing concentrations of xylose than the wild-type strain (Fig. 4d).

We also tested the susceptibility of a non-essential *A. fumigatus pkcA* mutant, carrying a Gly579Arg substitution juxtaposed to the PkcA C1B regulatory domain, as well as a Δ*rlmA* mutant to COL alone and in the presence of CAS (Fig. 5a). The *pkcA*^{G579R} mutation has a reduced activation of the downstream MpkA, resulting in the altered expression of genes encoding cell wall-related proteins, markers of endoplasmic reticulum stress, and the unfolded protein response[69,70].

https://doi.org/10.1038/s41467-025-60991-z

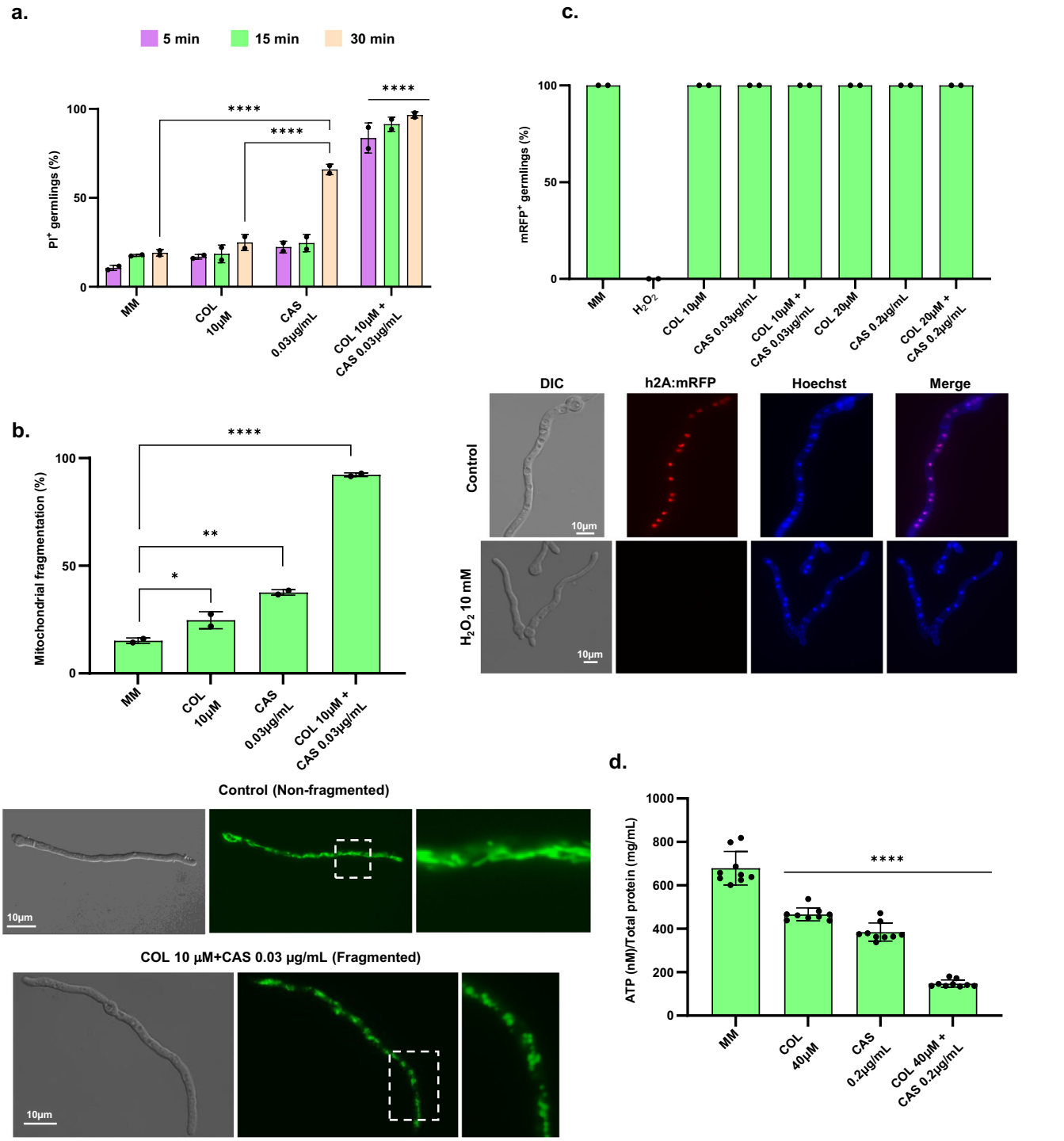

Fig. 3 | COL + CAS induces cell death. a *A. fumigatus* was grown for 16 h at 37 °C and exposed or not to either COL 10 μM, CAS 0.03 μg/mL, or the combination for 5, 15, and 30 min. Then, propidium iodide (PI) was added. The results show the percentage of germlings with co-localization of PI and Hoechst labeling (named as PI^+) and are expressed as mean values (%) of two independent experiments with at least 50 germlings per condition ($n = 100$ germlings) for each experiment ± SD. The data was statistically analyzed by the Two-way ANOVA and Tukey's multiple comparisons test (****$p < 0.0001$). **b** An *A. fumigatus* strain with mitochondria constitutively expressing GFP was grown for 16 h at 37 °C and exposed or not to either COL 10 μM, CAS 0.03 μg/mL, or the combination of both for 15 min. The results show the percentage of germlings with fragmented mitochondria, which are expressed as the average of two independent experiments with at least 30 germlings per condition for each experiment ($n = 60$). The results are expressed as mean values (%) of the two independent experiments ± SD. The data was statistically analyzed by the one-way ANOVA and Dunnett´s multiple comparisons test (*$p < 0.01$, **$p < 0.001$, and ****$p < 0.0001$). A representative image of non-fragmented and fragmented mitochondria is shown, scale bar = 10 μm. The white hatching in each image is amplified and shown as insets. **c** Fluorescence microscopy of *A. fumigatus* conidia containing the histone h2A::RFP exposed to H_2O_2 (10 mM), COL (10 or 20 μM), CAS (0.03 or 0.2 μg/mL), or different combinations of CAS + COL for one h at 30 °C. The germlings were assessed for Hoechst staining and RFP and the results are expressed as mean values (%) of the two independent experiments (50 germlings each experiment) ± SD. A representative image of the H_2O_2 treatment is shown, scale bar = 10 μm. **d** Total ATP production by *A. fumigatus* wild-type after growth for 24 h in MM at 37 °C and exposure to COL 40 μM, CAS 0.2 μg/mL or a combination of both compounds. The results are the average of three independent repetitions with three biological replicates each ($n = 9$) ± SD. The data was statistically analyzed by the Two-way ANOVA and Tukey's multiple comparisons test (****$p < 0.0001$). Source data are provided as a Source Data file.

https://doi.org/10.1038/s41467-025-60991-z

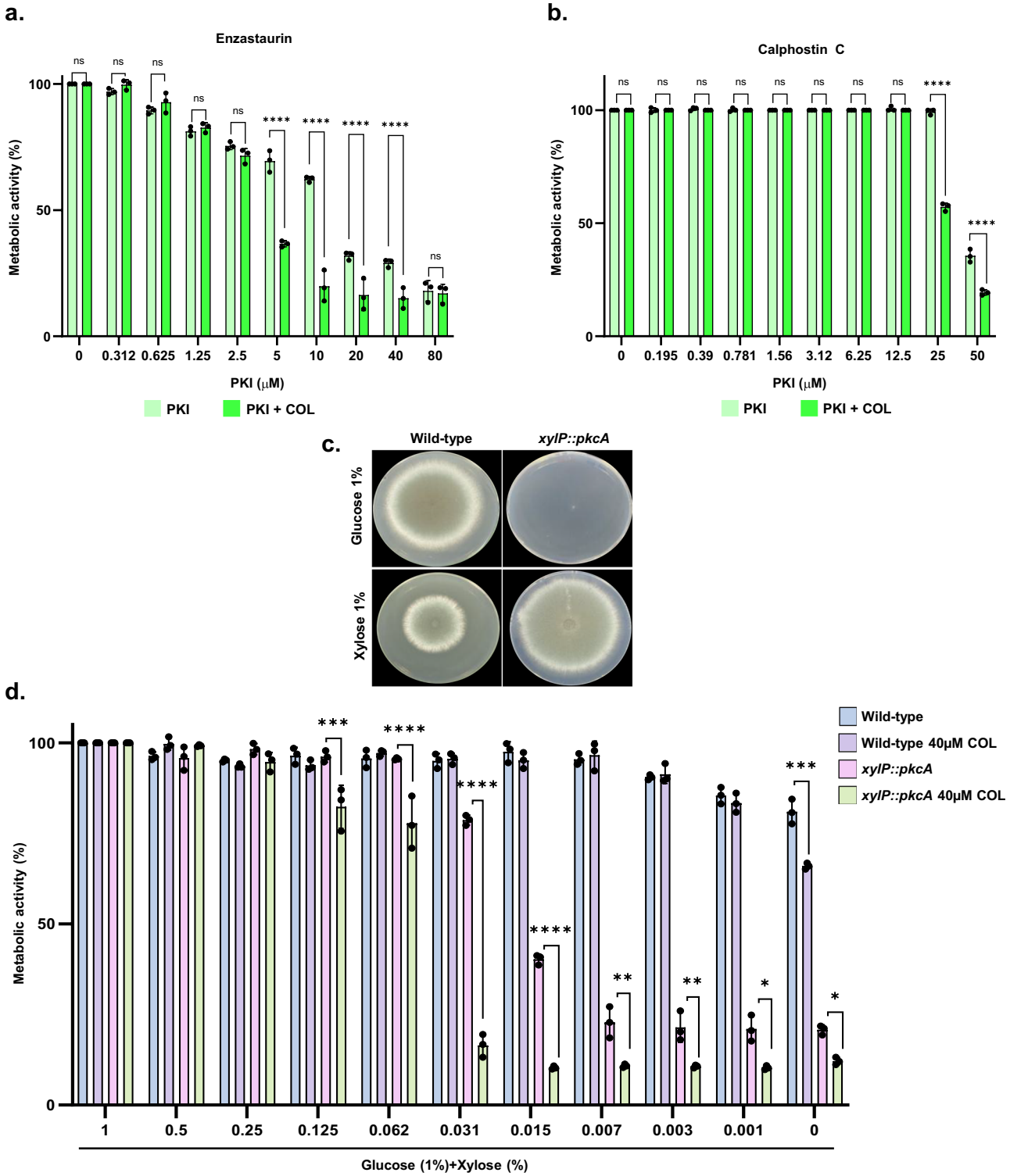

Fig. 4 | Protein kinase C is important for COL susceptibility. *A. fumigatus* was grown in liquid MM using 96-well plates at 37 °C in the presence of different concentrations of enzastaurin (**a**) and calphostin C (**b**) with or without 20 μM of COL, and after 48 h, the metabolic activity (%) was assessed by the XTT assay. The results represent the average of three independent experiments ± SD and were statistically analyzed by the Two-way ANOVA test ($n = 3$; $^{****}p < 0.0001$, ns: not significant). **c** *A. fumigatus* wild-type and *xylP::pkcA* strains were grown for 96 h at 37 °C in MM +glucose 1% and MM+xylose 1 %. **d** *A. fumigatus* wild-type and *xylP::pkcA* strains were grown for 48 h at 37 °C in MM+glucose 1% and supplemented with increasing concentrations of xylose, in the absence or presence of 40 μM COL. Metabolic activity was evaluated by using Alamar blue. The results are expressed as the average of three independent experiments ± SD. ($n = 3$; Two-way ANOVA, Tukey´s post-test; $^{*}p < 0.05$, $^{**}p < 0.005$, $^{**}p < 0.001$ and $^{****}p < 0.0001$). Source data are provided as a Source Data file.

https://doi.org/10.1038/s41467-025-60991-z

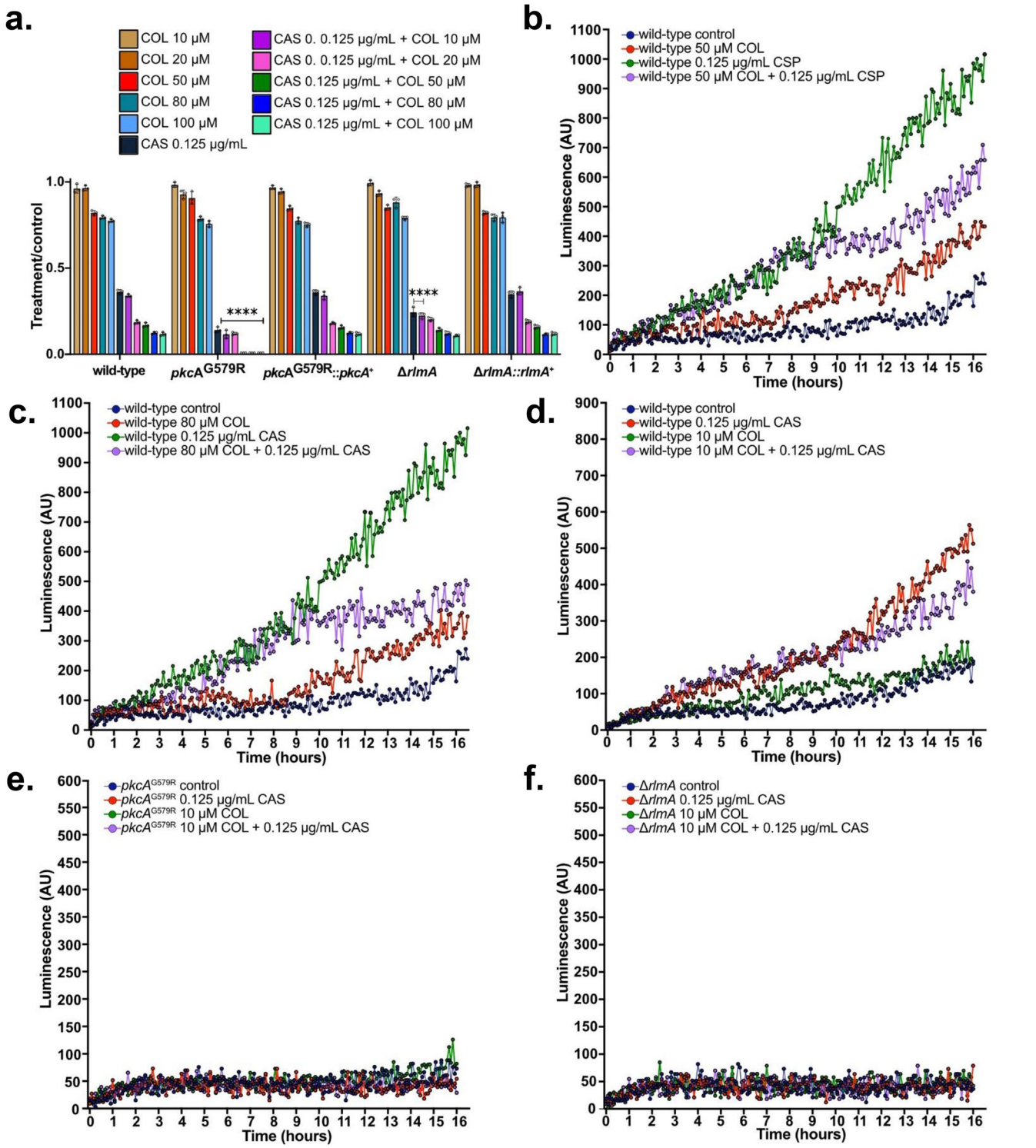

Fig. 5 | The Cell Wall Integrity Pathway is involved in the mechanism of action of COL + CAS. a *A. fumigatus* wild-type, *pkc*A^{G579R}, Δ*rlmA*, and complemented strains (5 µL with 1×10^4 conidia) were grown on solid medium with different treatments as indicated. The plates were incubated for 4 days at 37 °C, radial growth was measured, and the results are expressed as treatment/control ratio. Results were plotted using GraphPad Prism (GraphPad Software, Inc.) and are expressed as the average of three independent experiments ± SD. ($n = 3$; Two-way ANOVA, Dunnett´s post-test; $^{****}p < 0.0001$). **b**–**f**. Lux activity assay (luminescence, indicating luciferase activity) measured during incubation of *A. fumigatus* wild-type and mutant strains with *pagsA:mluc* cassette exposed to different concentrations of COL and/or CAS. The results were normalized by the number of conidia (1.5 × 10^4 per assay) and were repeated at least three times. The current graphs show representative experiments. Source data are provided as a Source Data file.

https://doi.org/10.1038/s41467-025-60991-z

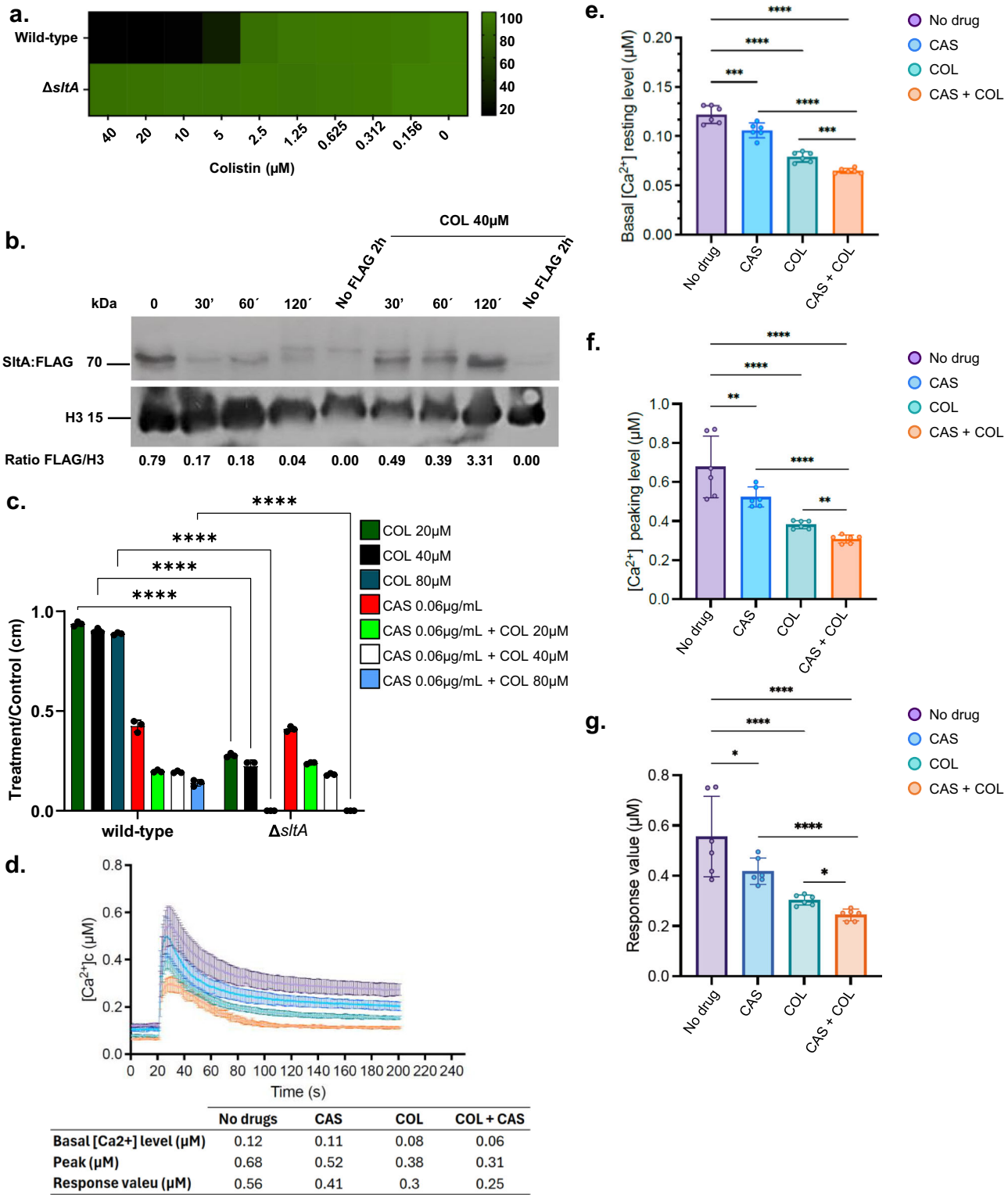

	No drugs	CAS	COL	COL + CAS
Basal [Ca2+] level (μM)	0.12	0.11	0.08	0.06
Peak (μM)	0.68	0.52	0.38	0.31
Response valeu (μM)	0.56	0.41	0.3	0.25

The *pkcA*^{G579R} mutant displayed reduced growth upon incubation with both CAS and COL alone and in the compound combination when compared to the wild-type strain or complemented strains (Fig. 5a). To evaluate if COL could activate the CWI pathway, we used a cassette with the promoter of the *agsA* gene (encoding the α-glucan-1,3-synthase from *A. niger*) fused with the luciferase gene (*mluc*) to monitor and measure temporal changes in *agsA* expression upon COL and/or CAS exposure. This approach was chosen because *A. fumigatus* PkcA activates the transcription factor RlmA, and the RlmA box domain [TA(A/T)4TAG] in the *agsA* promoter [*(p)agsA*] is required to induce the *agsA* gene in the presence of calcofluor white (CFW)[70,72]. We introduced the (p)*agsA::mluc* cassette into the wild-type, *pkcA*^{G579R} and Δ*rlmA* mutants (Fig. 5b, f). First, we determined the activity of the *(p)agsA* promoter in the presence of the cell wall damaging agent Calcofluor White (CFW) (Supplementary Fig. 3). As expected, the (p)*agsA::mluc* in the wild-type strain but significantly reduced when the mutant strains are exposed to CFW (Supplementary Fig. 3).

The luciferase activity of the wild-type strain was determined in the presence of different concentrations of CAS and COL (Fig. 5b, c). CAS (0.05 μg/mL and 0.125 μg/mL) induced luminescence readings ~4-

Fig. 6 | *A. fumigatus* transcription factor SltA is important for the MoA of COL. **a** *A. fumigatus* was grown in liquid MM using 96-well plates at 37 °C in the presence of different concentrations of COL. After 48 h, the metabolic activity % was assessed by the alamar blue assay. The results represent the average of two independent experiments. **b** Western blot showing the increased cleavage of SltA when the *A. fumigatus* SltA:FLAG strain is exposed to COL 40 μM. The WB are representative results from three independent experiments. **c** *A. fumigatus* wild-type, and Δ*sltA* strains (5 μL with 1×10^4 conidia) were grown on solid medium with different treatments as indicated. The plates were incubated for 4 days at 37 °C, radial growth was measured, and the values are expressed as treatment/control ratio. The results are the result of 3 independent experiments performed in duplicate ± SD. The data were statistically analyzed by the Two-way ANOVA test ($n = 6$; $^{****}p < 0.0001$ with Sidak's multiple comparisons test comparing the Δ*sltA*, mutant with the wild-type strain). **d**–**g**. The linear graphs indicate the real-time $[Ca^{2+}]_c$ changes in response to different drug stimuli (CAS 0.2 μg/mL, COL 20 μM, or the combination of CAS 0.2 μg/mL + COL 20 μM)$[Ca^{2+}]_c$, the free Ca^{2+} concentration in cytosol. Basal $[Ca^{2+}]$, the resting level prior to extracellular calcium stimulus. $[Ca^{2+}]$ amplitude, the peak value after the extracellular calcium stimulus. Response value, the difference between the basal $[Ca^{2+}]$ level and the poststimulatory peak value. The data are the average of eight (d) or six biological replicates (**e**–**g**.). Error bars show the SD. Statistical significance was determined by One-way ANOVA and a *t*-test ($^{*}p < 0.05$; $^{**}p < 0.01$; $^{***}p < 0.001$; $^{****}p < 0.0001$). Source data are provided as a Source Data file.

to 5-fold higher than no compound controls (Fig. 5b, c). COL (50 and 80 μM) also induced luminescence signal about 2-fold higher than no compound controls, indicating that the activation of this signaling pathway by COL is much less relevant compared to CAS, while the combination of COL with CAS induced readings in between CAS and COL only, suggesting an abrogation in the signaling emerging from the CWI pathway (Fig. 5a, b).

The wild-type showed 8- to 12- fold induction of luciferase activity when exposed to CAS 0.125 μg/mL or a lower dose of COL (10 μM), combined with CAS 0.125 μg/mL (Fig. 5d). In contrast, no luciferase induction in the *pkcA*^{G579R} mutant was detected when the potentiation caused by a low concentration of COL was applied to the mutant, culminating with the complete inactivation of the transcription factor RlmA, similar to the control condition where Δ*rlmA* strain was assayed under the same conditions (Fig. 5d, e). These results indicate PkcA is important for COL susceptibility in *A. fumigatus*, and both COL and CAS induce the CWI pathway in a PkcA dependent manner.

Screen of transcription factor mutant collection identifies SltA as important for COL susceptibility

To assess if any *A. fumigatus* transcription factors (TFs) play a role in COL MoA, a library of 484 *A. fumigatus* TF deletion mutants[73] was screened for sensitivity to COL (20 μM). We identified a single strain that was significantly hypersensitive to COL, a mutant harboring a deletion in the gene *sltA* (AFUB_041100) that encodes a C_2H_2 zinc finger TF[74–78]. The Δ*sltA* COL-susceptibility was further validated by metabolic activity (COL 0-40μM), increased expression of SltA when *A. fumigatus* SltA:FLAG was exposed to COL 40 μM (about 4-fold when compared to the non-exposure to COL for 2 h), and radial growth experiments that showed the Δ*sltA* strain is significantly more sensitive to COL than the corresponding wild-type strain (Fig. 6a–c). Interestingly, the Δ*sltA* mutant was not significantly different from the wild-type strain when grown in COL (20 or 40 μM) in the presence of CAS (0.06 μg/mL), suggesting the importance of this TF in the cellular response to COL (Fig. 6c). To further verify the relationship between COL and CAS with the expression levels of *sltA*, we tested a strain overexpressing *sltA* (mRNA level increased ~4-fold[78]; Supplementary Fig. 4). As previously shown, the Δ*sltA* strain had comparable growth with the wild-type in the presence of increasing CAS concentrations (0.03 to 0.15 μg/mL) and was more sensitive in the presence of COL (Supplementary Fig. 4a and 4b). Overexpression of *sltA* in the presence of CAS showed a comparable susceptibility to CAS but conferred 15% more tolerance to COL (80 μM) when compared to the wild-type strain (Supplementary Fig. 4a and 4b). There were no differences between the *sltA* ovexpression strain and the wild-type in the presence of different COL + CAS combinations (Supplementary Fig. 4b). These results emphasize the importance of SltA in the COL-susceptibility.

COL affects calcium availability through the calcineurin signaling pathway

In other pathogens, COL has been proposed to bind to cell membrane lipids, competitively displacing cations such as Ca^{2+} and Mg^{2+} that stabilize the membrane, resulting in permeabilization, leakage, and cell death[42]. Furthermore, deletion of *sltA* causes abnormal expression of calcium metabolism-related genes, resulting in decreased cytosolic Ca^{2+} under calcium-limited conditions[75]. Importantly, supplementation with exogenous calcium rescues the mutant phenotype[75]. Thus, we assessed the relationship of COL with calcium in *A. fumigatus*[42,47]. We used a combination of inhibitory concentrations of COL (5 μM) and CAS (0.2 μg/mL), and added different concentrations of Ca^{2+} (from 3.12 to 200 mM). We observed that addition of calcium restored *A. fumigatus* growth at concentrations as low as 3.12 mM (Supplementary Data 6), indicating externally supplied calcium can abolish the COL potentiation of CAS against *A. fumigatus*. To validate these findings, we monitored transient cytosolic Ca^{2+} levels in response to extracellular calcium by expressing codon optimized aequorin in living cells of *A. fumigatus*[79,80]. Upon treatment with 10 mM $CaCl_2$, the $[Ca^{2+}]_c$ (the free Ca^{2+} concentration in cytosol) in the wild-type strain transiently increased from a basal resting level of ~0.12 μM to a peak concentration of 0.68 μM and then gradually returned to a stable resting level (Fig. 6d). Thus, the difference of $[Ca^{2+}]_c$ between the peak and the resting status was about 0.56 μM (Fig. 6d). As shown in Fig. 6e, f, the basal resting level and peak level of $[Ca^{2+}]_c$ showed significant reduction when treated with CAS, COL, or the combination. Notably, the response value of $[Ca^{2+}]_c$ was 0.41 μM (~ 16% decrease), 0.3 μM (~ 12% decrease) compared to that of in wild-type cells upon exposure to COL + CAS (0.25 μM) (Fig. 6g). Collectively, these data suggest that *A. fumigatus* displays a significant decrease in intracellular calcium accumulation when exposed to the COL and CAS combination treatment.

Given the increased susceptibility to COL we observed with the Δ*sltA* mutant coupled with the decreased intracellular Ca^{+2} that occurs with COL treatment, we reasoned that COL is likely starving the Δ*sltA* mutant for Ca^{+2} that is required for its growth. To address this hypothesis, we grew wild-type and Δ*sltA* strains in MM supplemented with COL (40 μM), as well as different $CaCl_2$ concentrations (25–100 mM) (Fig. 7a, b). As previously shown, Ca^{+2} addition was able to improve Δ*sltA* radial growth allowing the mutant to grow comparable to the wild-type strain (Fig. 7a, b). More importantly, Ca^{+2} addition was also able to rescue Δ*sltA* growth in the presence of 40 μM COL, strongly indicating once more that COL MoA is related to Ca^{+2} availability to the fungal cell.

Considering that the protein phosphatase calcineurin signals through the calcium- and calcineurin-dependent TF CrzA, which binds to and regulates the expression of specific chitin synthase genes and other genes important for coping with CAS tolerance[81], we tested the susceptibility of Δ*calA* and Δ*crzA* to CAS (0.06 μg/mL) and CAS (0.06 μg/mL) in the presence of COL (20, 40, and 80 μM) (Fig. 7c, d). Interestingly, deletion of the catalytic subunit of calcineurin (*calA)* or *crzA* resulted in significantly better growth in CAS alone or with COL and CAS in combination compared to wild-type (Fig. 7c, d). Previously, it was demonstrated that a Δ*sltA* Δ*crzA* double mutant could grow better in higher calcium concentrations than the Δ*sltA* mutant alone[75]. However, the Δ*sltA* Δ*crzA* double mutant was as sensitive to COL and COL with CAS as Δ*sltA* alone (Fig. 7e), suggesting impairment of calcineurin signaling only rescues growth in the compound combination but not in the absence of *sltA*.

https://doi.org/10.1038/s41467-025-60991-z

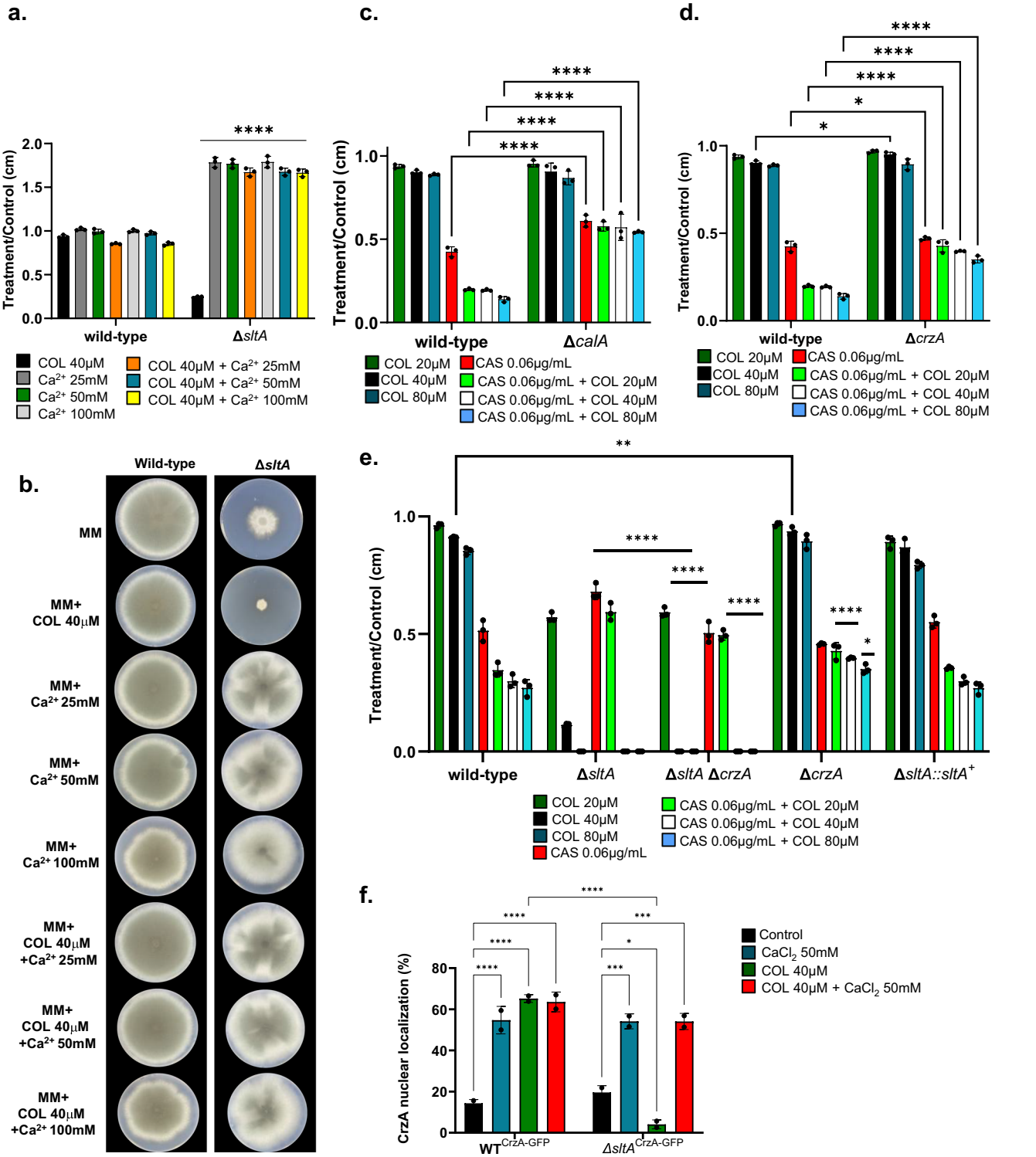

To further examine the link between these two transcription factors, we wanted to look at localization of CrzA upon compound exposure. When a wild-type strain was exposed to $CaCl_2$(50 mM) COL (40 μM), or $CaCl_2$ + COL (50 mM + 40 μM) for 15 min, CrzA:GFP translocation to the nucleus was increased about 4-fold (Fig. 7f). Similarly, in a Δ*sltA* background, localization of CrzA:GFP to the nucleus increased about 4-fold when the strain was exposed to either $CaCl_2$ (50 mM) or 5$CaCl_2$ with COL (50 mM + 40 μM). In contrast, there was a 3- to 4-fold reduction in CrzA:GFP localization relative to untreated when the Δ*sltA* was exposed to 40 MμCOL for 15 min (Fig. 7f). These results suggest once more that although calcium starvation is a very important component of the COL MoA against *A. fumigatus*, it is not the single COL MoA.

COL has therapeutic potential as a combination agent in *A. fumigatus*

The cytotoxicity of CAS with COL was assayed using the human immortalized epithelial cell lineage A549 (https://bcrj.org.br/, code 0033) and HepG2 liver immortalized cells (Fig. 8a, b). Confluent cultures of A549 or HepG2 cells were exposed to increasing concentrations of COL (0 to 80 μM) with or without CAS (100 μg/mL or 50 μg/mL) for 24 or 48 h, and cell viability was assessed by XTT or

Fig. 7 | The calcineurin signaling pathway is important for COL bioactivity. **a**, **b** *A. fumigatus* wild-type and Δ*sltA* strains were grown on solid MM without or with different treatments (COL 40 μM, $CaCl_2$ [25, 50, or 100 mM], or a combination of COL and $CaCl_2$). After 4 days at 37 °C, the radial growth was measured, and the values are expressed as treatment/control ratios. Results are expressed as the average of 3 independent experiments performed in technical duplicate ± SD. The data was statistically analyzed by the Two-way ANOVA test ($n = 6$; $^{****}p < 0.0001$ with Sidak's multiple comparisons test comparing the Δ*sltA*, mutant with the wild-type strain). **c**, **d** Conidia of *A. fumigatus* wild-type, Δ*calA*, and Δ*crzA* strains (5 μL with 1×10^4 conidia) were grown on solid MM or MM supplemented with COL (20 and 40 μM), CAS (0.06 μg/mL), or combinations of both compounds, as indicated. The plates were incubated for 4 days at 37 °C. The values are expressed as treatment/control ratios and show the average of 3 independent experiments performed in technical duplicate ± SD. The data was statistically analyzed by the Two-way ANOVA test ($n = 6$; $^{****}p < 0.0001$ with Sidak's multiple comparisons post-test). **e** *A. fumigatus* wild-type, Δ*sltA*, Δ*crzA*, Δ*sltA* Δ*crzA*, and Δ*sltA*:*sltA*$^+$ strains (5 μL with 1×10^4 conidia) were grown on solid MM either without any treatment or supplemented with 20 and 40 μM of COL, 0.06 μg/mL of CAS, or the combination of both, as indicated. The plates were incubated for 4 days at 37 °C. Results are expressed as treatment/control and show the average of 3 independent experiments performed in technical duplicate ± SD. The data was statistically analyzed by the Two-way ANOVA test ($n = 6$; $^{****}p < 0.0001$ with Tukey´s multiple comparisons post-test). **f** The CrzA:GFP and Δ*sltA* CrzA:GFP were grown for 16 h in liquid MM and transferred to $CaCl_2$ (50 mM), COL (40 μM), and $CaCl_2$ + COL (50 mM + 40 μM) for 15 min. CrzA:GFP nuclear translocation to the nucleus was analyzed. Hundred germlings were counted for each treatment, and the results are expressed as % of CrzA:GFP nuclear localization for germlings. Results represent the average of two independent experiments with at least 230 nuclei assessed in each assay ± SD. The data was statistically analyzed by the Two-way ANOVA test and Tukey´s post-test ($^{****}p < 0.0001$, $^{***}p < 0.0005$, and $^{*}p < 0.05$). Source data are provided as a Source Data file.

Alamar blue assays, respectively (Figs. 8a, b). In comparison to the control, when the cells were incubated with either CAS (100 μg/mL) or COL (from 0-80 μM), the drugs did not present significant levels of toxicity to A549 cells (Fig. 8a). The same lack of toxicity was observed with COL (0, 20, 40 and 80 μM) in the presence of CAS (100 μg/mL) (Fig. 8a). Comparable results were observed for HepG2 cells where toxicity was not observed with COL (0, 20 and 40 μM) in the presence of CAS (50 μg/mL) (Fig. 8b). Notice that positive controls like dimethyl sulfoxide (DMSO) or the anti-topoisomerase II agent topotecan showed very high toxicity to both cell lineages (Fig. 8a, b).

The ability of COL with CAS to promote the killing of *A. fumigatus* conidia cells in co-culture with A549 pulmonary cells was also evaluated. When A549 cells were exposed to VOR (0.5 μg/mL), the standard of care, as a control, *A. fumigatus* conidial killing reached 85% (Fig. 8c). By adding COL (20 and 40 μM) or CAS (50 μg/mL), the conidial killing reached from 25 to 45%. Encouragingly, the combination of COL (20 and 40 μM) with CAS (50 μg/mL) exposure showed about 55 to 75% *A. fumigatus* conidial killing (Fig. 8c). However, interestingly COL (80 μM) alone provides the same level of conidial killing than the combination of COL 80 μM + CAS 50 μg/mL, suggesting that COL (80 μM) is able to reduce the conidial survival.

We asked whether the combination COL + CAS could control *A. fumigatus* virulence. *Galleria mellonella* larvae were treated with PBS or infected with the *A. fumigatus* wild-type and the larvae were treated either with no drug, CAS (0.4 μg/mL), COL (40 μM) or COL (40 μM) + CAS (0.4 μg/mL) and survival was assessed over a time period of 8 days (Fig. 8d). There was no mortality in the larvae treated with PBS but larvae infected with *A. fumigatus* without any drug had 100% mortality after 7 days postinfection (p.i.) while larvae infected and treated either with CAS or COL had 90% and 80% after 8 days p.i., respectively (Fig. 8d). In contrast, larvae treated with a combination of COL + CAS had 40% after 8 days p.i. (Fig. 8d). *Caenorhabditis elegans* animals were infected with the *A. fumigatus* wild-type and the animals were treated either with water, CAS (0.4 μg/mL), COL (40 μM), or the combination and survival was assessed over a time period of 3 days (Fig. 8e). In animals infected with *A. fumigatus* and treated with water, there was 98.5% mortality observed after 3 days. While COL alone had no impact on *C. elegans* survival, CAS alone significantly improved survival, and importantly the compound combination significantly improved survival relative to single drug treatments or the untreated control (Fig. 8e). Taken together these data suggest that the combination COL + CAS is non-toxic to mammalian cells, it is able to enhance clearance of *A. fumigatus* infection in pulmonary cells in in vitro assays, and can also significantly decrease *A. fumigatus* infection in both the *G. mellonella* wax moth and *C. elegans* models of infection.

.

Discussion

CAS is defined as a fungistatic drug against *Aspergillus* because of its inability to kill entire hyphae, and acts by non-competitively inhibiting the enzyme β-1,3-glucan synthase, compromising integrity of the fungal cell wall[82]. The main morphological hallmarks that allow survival during exposure of *A. fumigatus* to CAS are: (i) lysis of the apical tips, (ii) containment of the lytic effect at the hyphal tip by the plugging of septal pores, and (iii) emergence of new hyphal tips behind blocked septa growing into or around lysed hyphal compartments[82–85]. As a result of these modifications, tolerance to CAS can be visualized and established as highly compacted hyperbranched microcolonies with increased septation and chitin content[81–87]. Further, we recently uncovered an endogenous mechanism of CAS tolerance in *A. fumigatus* whereby the inducible oxylipin signal 5,8-diHODE confers protection against tip lysis via the transcription factor ZfpA[85].

Molecules known to synergize with CAS against *A. fumigatus* include diphenyl diselenide and clofazimine[88,89]. Recently, we identified 11 compounds that can potentiate CAS, including the host defense peptide mimetic, brilacidin (BRI), which acts as a synergizer with CAS against CAS-sensitive and -resistant isolates of *A. fumigatus*, *Candida albicans*, *C. auris*, and CAS-intrinsically resistant *Cryptococcus neoformans*[36,90]. Here, by screening three repurposing libraries of 5,297 chemicals, we identified four compounds that can potentiate CAS: (i) LER, (ii) aprotinin, (iii) cyclic somatostatin, and (iv) COL. Except for aprotinin, which is a protease inhibitor commonly used against viral respiratory diseases[48], all other compounds are known to affect different aspects of calcium homeostasis. LER is a calcium channel blocker and it is used to treat hypertension[47]; cyclic somatostatin binds to G-protein coupled receptors (GPCRs), decreasing intracellular cyclic AMP and calcium while simultaneously increasing outward potassium currents[49]; and COL binds the anionic lipopolysaccharide (LPS) molecules by displacing Mg^{2+} and Ca^{2+} from the outer cell membrane of Gram-negative bacteria, leading to permeability changes in the cell envelope and leakage of cell contents[51]. The combination of LER with CAS and COL with CAS was able to convert CAS into a fungicidal drug.

Upon CAS exposure, *A. fumigatus* calcium-calmodulin signaling activates the calcium responsive transcription factor CrzA via dephosphorylation by calcineurin[81,91–93]. Dephosphorylated CrzA translocates into the nucleus to induce the expression of chitin synthase genes to increase chitin production, which is essential for CAS tolerance[81,86]. Since LER, cyclic somatostatin, and COL can affect calcium homeostasis, it is possible the main MoA of these compounds as synergizers of CAS is related to calcium depletion, blocking either the calcium entrance into the cell and/or its release from cellular organelles where it is stored. This calcium depletion effect of COL with CAS was confirmed when we used a functional *A. fumigatus* aequorin strain. COL in combination with azoles and echinocandins has already been reported

https://doi.org/10.1038/s41467-025-60991-z

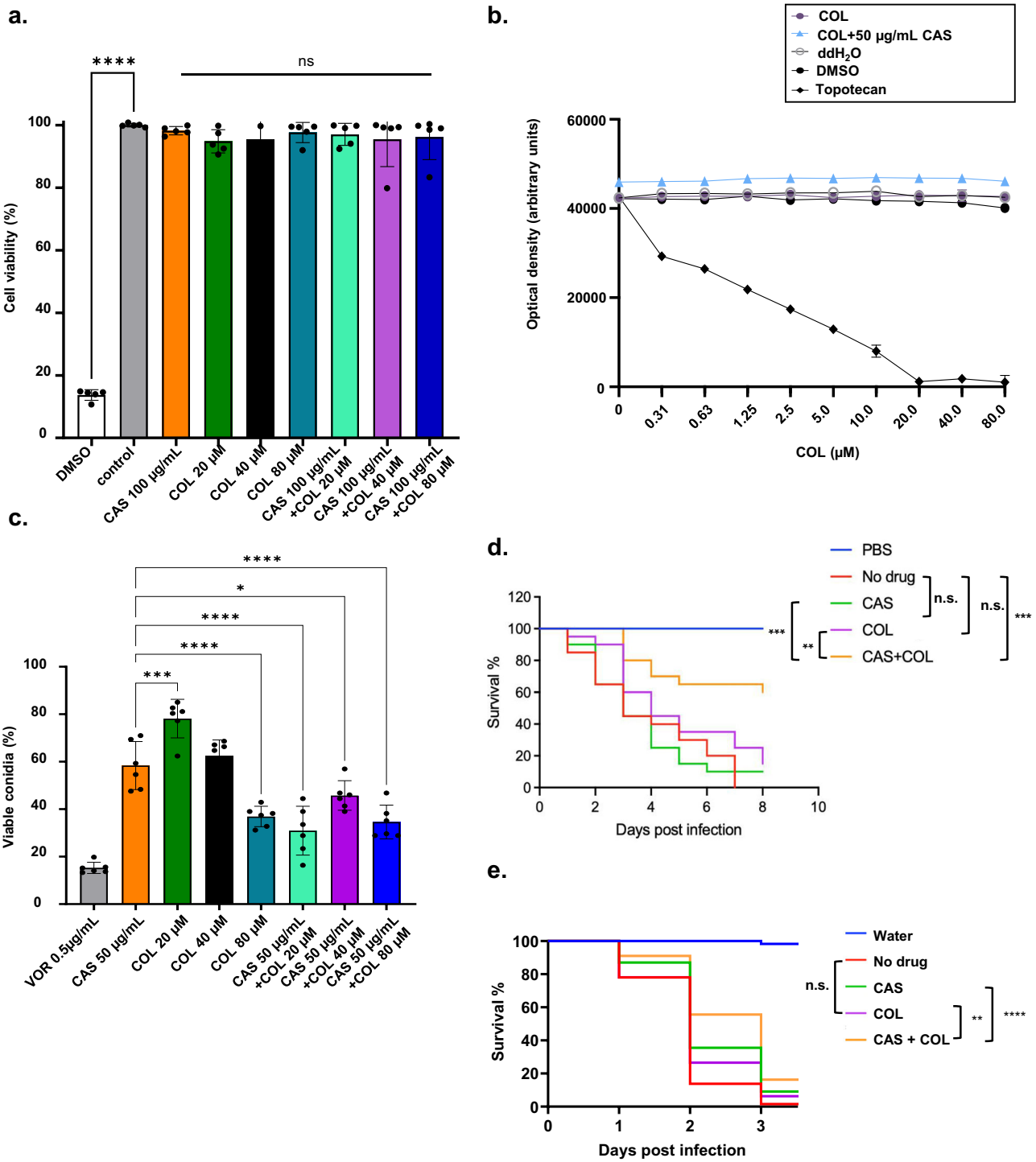

to have a synergistic effect against important pathogenic fungi like *Candida* spp[37–46]., *C. neoformans*[37,40], *A. nidulans*, *A. niger*, and *A. terreus*[44,45,94]. Combinations of COL with other azoles or with CAS against *A. fumigatus* have not been investigated; however, COL has synergized amphotericin B against *A. fumigatus*[45,95].

We focused on defining the MoA of COL as a CAS synergizer. COL is a bactericidal antibiotic used against Gram-negative bacteria[50,96]. It is a polycationic peptide and has both hydrophilic and lipophilic moieties[50,96]. These cationic regions interact with the bacterial outer membrane binding to lipopolysaccharides (lipid A) and phospholipids where it competitively displaces divalent cations (Ca^{2+} and Mg^{2+}) from the phosphate groups of membrane lipids. This leads to disruption of the outer cell membrane, leakage of intracellular contents, and bacterial death[50,96]. The hydrophobic and hydrophilic regions interact with the cytoplasmic membrane solubilizing the cell membrane[50,96]. Although COL is not an antimicrobial peptide, its net effect against *A. fumigatus* could be compared to an antimicrobial peptide that targets directly or indirectly the fungal plasma membrane, disrupting its membrane potential[97,98]. COL can synergize CAS, ANID, and IBX against *A. fumigatus* but not VOR. COL has antagonistic interaction with MYR (a specific inhibitor of the serine palmitoyl transferase, the first step in the sphingolipid biosynthesis) suggesting that COL is impacting cell membrane organization. Actually, exposure of *A. fumigatus* germlings to COL with CAS increases membrane permeability and mitochondrial fragmentation as well as reduces ATP production as a read out of mitochondrial activity, indicating the fungicidal effect of COL and CAS

https://doi.org/10.1038/s41467-025-60991-z

Fig. 8 | COL and COL + CAS are not toxic to A549 pulmonary epithelial cells and COL + CAS decreases the *A. fumigatus* fungal burden. a A549 pulmonary epithelial cells were treated with CAS (100 μg/mL), COL (20, 40, 80 μM) or a combination of CAS + COL. After 48 h, cell viability was evaluated by the XTT assay. Positive and negative controls were 10% DMSO and untreated cells, respectively. The results show the average of five biological replicates ±SD. The data was statistically analyzed by the ordinary two-way ANOVA and Tukey´s post-test ($n = 5$; $^{****}p < 0.0001$ ns: not significant). **b** HepG2 liver cells were treated with 50 μg/mL of CAS, and 0 to 80 μM of COL alone, and in combination with 50 μg/mL of CAS, and after 48 h, cell viability was evaluated by Alamar blue assay. Positive and negative controls were topotecan, DMSO, and double-distilled (dd) water, respectively. The results represent the average of two independent experiments performed in technical triplicate ± SD ($n = 6$). **c** *A. fumigatus* conidial viability after infecting A549 pulmonary epithelial cells (MOI 1:10). After 24 h of incubation in 5% CO2, the culture media were removed, the wells were washed, the A549 cells were lysed, and the cell suspension was collected. This suspension was then diluted and plated on Sabouraud Dextrose Agar Media (SAB). After 48 h incubation at 37 °C, the number of colony-forming units (CFUs) was determined. VOR was used as a positive control. The results represent the average of three independent experiments performed in technical duplicate ($n = 6$). Data was statistically analyzed by the ordinary two-way ANOVA and Dunnett´s post-test ($^{****}p < 0.0001$; $^{***}p < 0.0005$, and $^{*}p < 0.05$). **d** Survival curves of *G. mellonella* larvae infected and treated (PBS, COL 40 μM, CAS 0.4 μg/mL or a combination of COL 40 μM + CAS 0.4 μg/mL). Uninfected and PBS-treated larvae were used as a negative control. The results are the combination of two independent experiments with 10 animals in each treatment ($n = 20$). Statistical differences between groups were determined using a log-rank test. $^{**}p < 0.01$; $^{***}p < 0.001$; ns, not significant. **e** Survival curves of *C. elegans* infected and treated (water, COL 40 μM, CAS 0.4 μg/mL or a combination of COL 40 μM + CAS 0.4 μg/mL Uninfected and water-treated larvae were used as a negative control. Log-Rank (Mantel-Cox) was used to determine the significance between Kaplan-Meier survival curves. The results are the combination of two independent experiments with 61 and 68 (water), 63 and 60 (COL), 51 and 79 (CAS), and 54 and 62 (COL + CAS) animals in each treatment. Statistical differences between groups were determined using a log-rank test. $^{**}p < 0.01$; $^{***}p < 0.001$; ns, not significant. Source data are provided as a Source Data file.

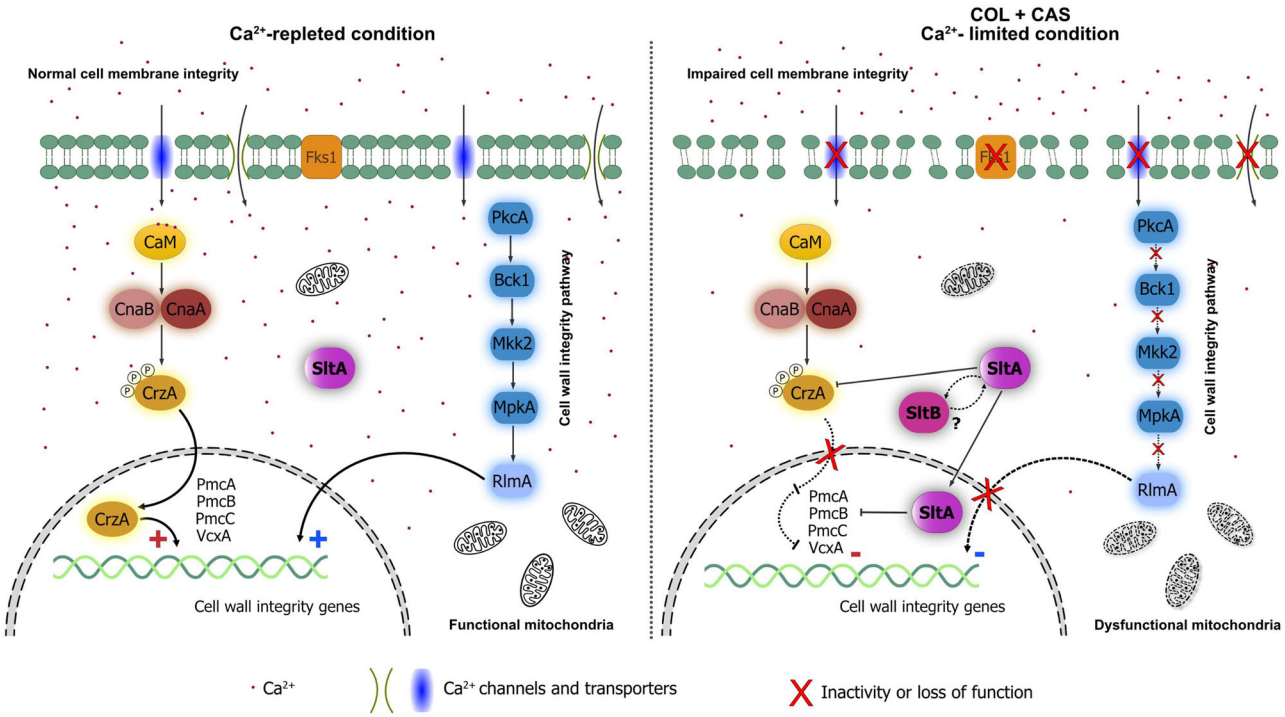

Fig. 9 | Model for the proposed MoA of COL + CAS that ensures loss of cell viability. In calcium-repleted conditions (left panel), calcium channels and transporters allow calcium transport into the cytoplasm, activating calcium sensors, like calmodulin (CaM), that bind to the regulatory subunit of calcineurin (CnaB), releasing the phosphatase activity of the catalytic subunit of calcineurin (CnaA). CnaA dephosphorylates the transcription factor CrzA that is translocated to the nucleus, turning on (+) the expression of the vacuolar calcium transporter-encoding gene *pmcA-C* and the vacuolar Ca^{2+}/H^{+} exchanger-encoding gene *vcxA* to avoid the excessive vacuolar storage of calcium and genes for stress responses and cell wall modifications. The cell wall integrity pathway comprises PkcA (protein kinase C), the mitogen-activated kinases (MAPK), MAPKKK (Bck1), MAPKK (Mkk2), and MAPK (MpkA), which are functionally and sequentially phosphorylated, allowing the phosphorylation and activation of RlmA transcription factor in the nucleus (+ sign). Active RlmA enables the transcription of enzymes responsible for the biosynthesis and/or remodeling of the cell wall (not shown in the Figure). One of them is α-glucan synthase 1 (not shown), which was used as a proxy for the RlmA-regulated network in the luciferase reporter assays. Another possible candidate is *fks1*, which encodes the β-1,3-glucan synthase, the enzyme responsible for the biosynthesis of β−1,3-glucan, the main polysaccharide in the *A. fumigatus* cell wall. and the molecular target of CAS. Mitochondria are intact and functional during these processes. Calcium-limited conditions (right panel) are induced promptly upon exposure of the cells to COL + CAS. Non-competitive inhibition of Fks1 imposed by CAS inhibition results in a decrease in the β−1,3-glucan content in the cell wall. The lack of this polysaccharide weakens the cell wall and increases the impact of osmotic pressure, disrupting the plasma membrane integrity pathway. Combination of COL + CAS inhibits PkcA signaling and impairment of RlmA output. The transcription factor SltA plays a dual role in maintaining calcium homeostasis under calcium-limited conditions. *A. fumigatus* SltA transcription factor is activated upon a proteolysis modification that depends on SltB, a chymotrypsin-like serine protease. It is currently unknown how SltB is regulated (question mark). SltA represses the expression and nuclear localization of CrzA, probably by affecting the activity of calcineurin, decreasing the expression and activity of calcium channels and transporters in the cell membrane (- sign). SltA regulates the expression of *pmcA*, *pmcB*, *vcxA*, and the Golgi calcium transporter-encoding gene *pmrA* by directly binding to the conserved AGGCA motif in their promoter regions. SltA can regulate the expression of *pmcC* and the mitochondrial calcium transporter-encoding gene *mcuA* in an indirect manner (not shown). The combination of COL + CAS impairs the function of CWI, plasma membrane integrity, and SltA, resulting in a cell death process through a combination of calcium starvation, increased leakage of cytoplasmic contents, and non-functional mitochondria due to enhanced fragmentation. The figure was created using the software Affinity Designer 2 (version 2.6.2).

is an apoptosis-like cell death. We demonstrate that combinations of COL and CAS are not toxic to human cells and increase the efficiency of conidial killing by lung epithelial cells, and survival in *G. mellonella* and *C. elegans*. COL can also potentiate IBX against *A. fumigatus* CAS-resistant strains. Interestingly, *A. fumigatus* CAS-resistant mutants that have a mutation in the *fks1* gene are not resistant to IBX, suggesting that these substitutions at S678P and S679P are not able to confer IBX resistance, supporting previous findings that have shown that an *A. fumigatus fks1* S679P strain is not resistant to IBX[99]. These results are also similar to *Candida* spp because IBX's binding site seems to be partially divergent from that of the echinocandins as IBX is active against echinocandin-resistant *Candida* isolates[100,101].

By using a combination of chemical genomic and functional genomic screens to identify *S. cerevisiae* and *A. fumigatus* mutants with altered sensitivity to COL, we identified many genetic determinants that affect cell permeability, regulate salt tolerance, and are involved in calcium metabolism. *A. fumigatus* protein kinase C and the TF SltA were identified as important COL effectors. PkcA is the apical kinase that activates the CWI pathway that culminates with the MpkA translocation to the nucleus, and the transcriptional modulation of several genes important for cell wall remodeling[66,102]. SltA is involved in conidial formation and germination, hyphal development, cell wall architecture, secretion of mycotoxins and secondary metabolites, the regulation of azole resistance, and most importantly, it confers adaptation to calcium-limited conditions[74–78]. The identification of the *sltA* deletion strain in a screen for mutants sensitive to COL established a solid ground for the hypothesis that COL disrupts calcium metabolism in *A. fumigatus*. This was confirmed by rescuing the Δ*sltA* COL-sensitivity by adding calcium to the growth medium. We propose a model where COL and CAS affect cell permeability, activating an intense cross-talk between PkcA and calcineurin that modulates a cascade of responses involving the TFs CrzA, RlmA, and SltA (Fig. 9). The gene targets that are under the control of these TFs will collaborate to strengthen the cell wall to avoid cytoplasmic leakage and cell death. However, the concomitant activity of COL and CAS bypasses these stress signaling pathways, which leads to cellular death (Fig. 9). Our work opens the possibilities of using COL and CAS as a possible therapy and an alternative to combat aspergillosis.

Methods

Ethical statement

The principles that guide our studies are based on the Declaration of Animal Rights ratified by UNESCO on January 27, 1978 in its 8th and 14th articles. All protocols adopted in this study were approved by the local ethics committee for animal experiments from the University of São Paulo, Campus of Ribeirão Preto (Permit Number: 23.1.547.60.8; Characterization of virulence and immunopathogenicity of *Aspergillus spp* in the murine model).

Media and strains

The *Aspergillus* spp. used in this work are listed in Supplementary Data 7. All *Aspergillus* strains were grown in either solid minimal medium (MM; 1% [wt/vol] glucose, 50 mL of a 20x salt solution, 1 mL of trace elements, 2% [wt/vol] agar, pH 6.5) or liquid MM (same composition as solid MM but without agar) at 37 °C. The composition of the trace elements and nitrate salts is described by Käfer[103].

Library drug screenings

Three different drug libraries were screened for antifungal activity against *A. fumigatus* CEA17 strain: Pharmakon (1600 compounds; http://www.msdiscovery.com/pharmakon.html), MedChem Express (2592 compounds; https://www.medchemexpress.com/), and LifeArc (1105 compounds; https://www.lifearc.org/). A total of 5297 compounds were screened to identify candidates that synergize with CAS against *A. fumigatus*. For the primary screening, 96-wells microplates were used, where each compound was added per well at a concentration of 20 μM, diluted in DMSO, in 100 μL of liquid MM with 10^4/mL spores, in the presence or absence of 0.2 μg/mL of CAS. After 48 h of incubation at 37 °C without agitation, growth was determined visually, and compounds with less than 20% of growth were selected for validation. As negative control, wells with only MM and DMSO were used. These experiments were done in duplicate. Validation was performed using alamar blue (Life technologies) to measure the inhibition of *A. fumigatus* metabolic activity by the selected compounds by themselves or in combination with CAS. Briefly, 100 μL of liquid MM with 2.5×10^4 conidia/mL supplemented or not with 0.2 μg/mL CAS plus an increasing concentration of each selected compound (0 to 80 μM) and 10% of alamar blue were grown in 96-well plates for 48 h at 37 °C. As a positive control, the drugs were replaced by the same volume of the medium, and as a negative control, 90 μL of liquid MM plus 10 μL of alamar blue were used. The plates were read spectrophotometrically by fluorescence (570 nm excitation-590 nm emission) in a microplate reader (SpectraMax Paradigm Multi-Mode Microplate Reader; Molecular Devices). Results are expressed as means ± standard deviation (SD) from two independent experiments performed by duplicate.

Luria-Delbruck fluctuation assay

Fluctuation assays were conducted as previously described by adding some modifications[66,104]. Briefly, ten independent *A. fumigatus* colonies were selected from a MM agar stock and cultured for four days in MM plates at 37 °C. Conidia were collected in sterile water + 0.01% Tween-20 and 1×10^{10} conidia were inoculated on plates with voriconazole or COL + CAS for 10 days at 37 °C; colonies were counted following incubation for 4 (control RPMI-1640 medium) or 14 days (drug media). Data from the fluctuation assay was analysed using the R package flan v0.9[105]. The analysis was conducted with default parameters, employing a 95 percent confidence interval for the mutation probability and the maximum likelihood method.

S. cerevisiae chemical genomics analysis

Chemical genomics analysis using *S. cerevisiae* mutant libraries was conducted as described[63,64]. The libraries include temperature-sensitive (TS), overexpression (MoBY), and diploid heterozygous deletion (HET) collections. A haploid deletion collection (ScWG: *Saccharomycescerevisiaewhole* genome), which is a barcoded collection of ~3500 haploid non-essential gene deletions in the drug hypersensitive strain (Y13206: *MATα snq2Δ::KlLEU2 pdr3Δ::KlURA3 pdr1Δ::NATMX can1Δna11::2iSp_his5 lyp1Δ his3Δ1 leu2Δ0 ura3Δ0 met15Δ LYS2*), was also constructed using SGA technology (manuscript in preparation) and used for chemical genomics analysis. Pooled yeast mutant libraries were treated with colistin. Basically, the workflow including culture, DNA extraction, and PCR amplification of each strain-specific barcode proceeded as described in[63]. Purified PCR products were sequenced with an Illumina Miseq machine at the RIKEN Center for Brain Science (Wako, Japan).

Minimum inhibitory concentration (MIC)

Once the selected compounds were validated by alamar blue, the MIC was determined based on the M38-A2 protocol of the Clinical and Laboratory Standards Institute[106]. Briefly, the assay was performed in 96-wells plates containing 100 μL of MM with 10^4 conidia/mL of different *Aspergillus* strains and increasing concentrations of the compound by itself (ranging from 0 to 80 μM) or in combination with 0.2 μg/mL of CAS. Plates were incubated at 37 °C without shaking for 48 h and the inhibition of growth was evaluated. The MIC was defined as the lowest drug concentration that visually attained 100% of fungal growth inhibition compared to the control well. Wells containing only MM and DMSO were used as controls. To determine if the compound or the combination of the compound with CAS had a fungistatic or

fungicidal effect, the plates were centrifuged, the supernatant was removed, and the cells were resuspended in water and then plate in solid MM and grow at 37 °C for 48 h. The number of viable colonies was determined by the CFU number compared to the negative control (no drug), which had 100% of survival. Results are expressed as means ± SD from three independent experiments performed by triplicate.

Checkerboard assays

To assess the interaction (synergistic, additive, or antagonistic) between the selected compounds and CAS, checkerboard assays were performed. Briefly, a stock solution of 2.5×10^4 spores/mL and 80 µM of the compound or 4 µg/mL of CAS were prepared in MM with 10% of alamar blue. In 96-wells microtiter plates, CAS was diluted sequentially along the ordinate, while the selected compound was diluted along the abscissa, to obtain a final volume of 100 µL. The plates were incubated for 48 h at 37 °C and the metabolic activity was determined by reading in the spectrophotometer as previously described. Results are expressed as means ± SD from three independent experiments. Combinations of the selected compounds with other drugs were also used, including CER and MYR. To determine the type of drug interaction, the SynergyFinder software[52] was used with the following parameters: detect outliners; yes; curve fitting: LL4; method: Bliss; correction: on. The summary synergy score represents the average excess response due to drug interaction, in which a value less than −10 suggest an antagonistic interaction between two drugs; values from −10 to 10 suggest an additive interaction; and values larger than 10 suggest a synergistic interaction.

Calcium assays

A combination of COL (5 µM) or LER (7.8 µM) plus CAS (0.2 µg/mL), an inhibitory concentration, and 10^4 spores/mL supplemented with different concentrations of Ca^2 + (0 to 200 mM) in MM was grown in 96-wells plates at 37 °C. After 48 h, the plates were analyzed visually to determine the concentration of Ca^{2+} in which the *A. fumigatus* growth was restored.

Measurement of the free Ca^{2+} concentration ($[Ca^{2+}]_c$)

The strain YJ35 (WT^{Aeq}, Δ*ku80;pyrG1*; *AMA1*::*PgpdA*::*Aeq*::*pyr4*) expressing aequorin was cultured for 2 days to form fresh spores. The spores were filtered through nylon cloth and washed 10 times in distilled deionized water. Ten million (10^7) spores in 100 µl liquid minimal medium were inoculated into each well of a 96-well microtiter plate (Thermo Fischer). The plate was incubated at 37 °C for 17 h. The medium was then removed gently with a pipette, and the cells in each well were washed twice with 150 µl PGM (20 mM PIPES pH 6.7, 50 mM glucose, 1 mM $MgCl_2$). Aequorin was reconstituted by incubating mycelia in 100 µL PGM containing native coelenterazine (2.5 µM) (Sigma-Aldrich, C-7001) at 4 °C for 4 h in the dark and then allowed to recover at 37 °C for 1 h. The medium was removed gently. Next, 2 µg/mL caspofungin (CAS) and/or 20 µM colistin was used as drug treatment and co-incubated with mycelia at 37 °C for 1 h. After removing the medium, luminescence was measured with an LB 960 Microplate Luminometer (Berthold Technologies, Germany), which was controlled by a dedicated computer running the MikroWin 2000 software. At the 20-s time point of luminescence reading, 10 mM $CaCl_2$ was applied as a stimulant. At the end of each experiment, the active aequorin was completely discharged by permeabilizing the cells with 20% (v/v) ethanol in the presence of an excess of calcium (2 M $CaCl_2$) to determine the total aequorin luminescence of each culture. The conversion of luminescence (relative light units [RLU]) into $[Ca^{2+}]$ was performed with using Excel 2023 software (Microsoft). Input data were converted using the following empirically derived calibration formula: pCa = 0.332588 (-log k) + 5.5593, where k is luminescence (in RLU) s^{-1}/total luminescence (in RLU).

ATP determination (luciferin-luciferase assay)

A. fumigatus conidia (1×10^8) wild-type strain were grown in 100 mL of liquid MM for 24 h at 37 °C followed by the treatment with COL (40 µM), CAS (0.2 µg/mL) or the combination of both for 4 h. Mycelia were then snap-frozen in liquid nitrogen, ground using mortar and pestle and resuspended in lysis buffer (10 mM Tris based, pH 7.5 buffer containing 0.1 M NaCl, 1 mM EDTA, 0.01% Triton X−100). Extracts were centrifuged at 13,000 × g for 10 min at 4 °C. The supernatants were collected and the total protein abundance was quantified using Bradford reagent (Bio-Rad). The ATP Determination Kit (A22066, Invitrogen) was employed for the luciferin-luciferase assay according to the manufacturer's instructions. To each well in a 96-well white plate, the kit reaction solution was added to the samples or standard solution provided by the kit at room temperature. For measurement of the ATP content, the luminescence of samples and standards was detected after 5 min of incubation in a Synergy-HT microplate reader (Bio-Tek) at 560 nm of emission. ATP concentrations (nM) were determined relative to the total protein content of the samples (mg/mL).

Luciferase reporter strains construction

The CRISPR-Cas9 methodology previously described for *Aspergillus*[107–109] was employed to insert the (p)*ags*A::*mluc* cassette into the *safe haven* (*Sh*) locus of the wild-type (Δ*aku*B^{KU80}), Δ*rlm*A and *pkcA*^{G579R} *A. fumigatus* strains[69,70]. The Sh locus was recently described as a site for inserting gene cassettes without interfering with the global expression program of the fungus[110,111]. The (p)*agsA::mluc* cassette was amplified from the MAF 6.6 strain[70] using the IM-g35 (5′-GCAGGA GCAAAAACAGGCCGGGAAGATATTGCCTAGGAGTTCTGCGCTGGCTC TAGAACTAGTGGATCCCC-3′) and IM-g36 (5′-CTGACAGTTCATGGA ATAGTAGAATGGTATGATACATTACGTAACCGACCCTAGAAAGAAGG ATTACCTCTAAAC-3′) primer pairs, which harbor 5´ and 3´ homology regions (50 bp) to the *A. fumigatus* Sh. For the CRISPR-Cas9 constructs, two protospacers consisting of 20 nucleotides upstream of the PAM previously identified by[111] were fused to the RNA backbone and the glycine tRNA amplified from pAC902[107,109] plasmid using Phusion U DNA polymerase (Thermo Scientific). The independent fragments obtained by PCR were then cloned into the CRISPR vector pFC332[107] using the USER cloning method (New England Biolabs), following the previously described methodology[109,112]. The pFC332 vector contains the *Aspergillus*-optimized coding sequence of the Cas9 nuclease gene, the AMA1 sequence that confers episomal self-replicative capability to the plasmid, as well as the hygromycin resistance gene for the selection of candidates in *A. fumigatus*. Hygromycin resistant transformants were validated by the presence of the (p)*ags*A::*mluc* DNA cassette in the Sh locus by PCR using the IM-745 (5′-CGTCCAACATCAGCGTCATG-3′) and IM-746 (5′-TCCGTTCCATTACGCCTTCC-3′) primers which are located upstream and downstream, respectively of the PAM and the site cassette insertion.

Luciferase activity assay

For the luciferase activity assay[70], 50 µl of 2 × MM with 0.006% yeast extract (w/v) and 50 µl spore suspension (3×10^5 conidia/ml) was pipetted together (in at least 12-replicates for each condition) in a well of a white 96-well plate (Greiner Bio-one) and incubated for 5 h at 37 °C. Thereafter, 50 µl of 2 × MM with 0.006% yeast extract (w/v), 26 µl deionized water, 4 µl 25 mM luciferin (Promega, E1605), and 20 µl of different concentrations of freshly dissolved colistin (Sigma) and/or caspofungin (Sigma) were added and subsequently incubated at 35 °C in the SpectraMAX i3 (Molecular Devices) with continuous measuring of luciferase luminescence for 16 h. The experiments were performed in at least three biological replicates. Graphs were plotted using GraphPad Prism 10.

mito::GFP strain construction

The mito::GFP strain was constructed through the gene replacement cassettes approach using 'in vivo' recombination in *S. cerevisiae* as previously described by[113]. Briefly, about 1.0 kb from the 5'-UTR of the pyrG gene was amplified (primers P1/P2) from *A. fumigatus* genomic DNA (gDNA). The gpdA sequence was amplified from gDNA of the *A. nidulans* AGB655 strain (primers P3/P4). The 5'- UTR of the citrate synthase gene was PCR amplified from *A. niger* gDNA (primers P5/P6), the GFP sequence was PCR amplified from pMCB17apx plasmid (provided by Vladimir P. Efimov; primers P7/P8) and the pyrG gene was amplified from the *A. fumigatus* gDNA (primers P9/P10). The cassette was generated by transforming each fragment along with the plasmid pRS426 linearized with *Bam*HI/*Eco*RI into the *S. cerevisiae* strain SC9721 using the lithium acetate method[114]. The DNA from the transformants was extracted by the method described by[115] and PCR were run to confirm the correct construction. The whole cassette was then PCR-amplified from *S. cerevisiae* DNA (primers P1/P9) and used to transform *A. fumigatus* strain[116]. *A. fumigatus* candidates were selected and purified through three rounds of growth on plates. The gDNA of the mutants was extracted and the construction insertion was confirmed by PCR (primers P11/P6). To note, all DNA fragments were PCR-amplified with TaKaRa Ex Taq DNA Polymerase (Clontech USA) and primers P1 and P9 contained a short homologous sequence to the MCS of the plasmid pRS426. A list of all primer pairs is shown in Supplementary Data 8.

Western blot analysis

A. fumigatus SltA:FLAG was grown in liquid MM for 16 h at 37 °C, and transferred or not to 40 μM of Colistin for 0, 0.5, 1 and 2 h. Wild-type strain was used as the control group (no FLAG). Total cellular protein extractions were carried out and quantified using Bradford reagent (Bio-Rad), according to manufacturer's instructions. 50 μg of protein from each sample were resolved in a 12% (w/v) SDS–PAGE and transferred to polyvinylidene difluoride (PVDF) membranes (Merck Millipore)[93]. FLAG-tagged proteins were detected using anti-mouse FLAG (1:5000, Sigma-Aldrich Co.) The primary antibody was detected using a secondary antibody anti-mouse IgG HRP conjugate (Cell Signaling Technology), at 1:10,000 dilution. Chemoluminescent detection was achieved using an ECL Prime Western Blot detection kit (GE HealthCare). To detect these signals on blotted membranes, the ECL Prime Western Blotting Detection System (GE Helthcare, Little Chalfont, UK) and LAS1000 (FUJIFILM, Tokyo, Japan) were used. The quantification of the signal intensity ratio of SltA-FLAG protein was performed using ImageJ.

Protein Kinase inhibitors (PKIs) screening

A collection of 58 PKIs was screened to assess their effect on *A. fumigatus* growth and metabolic activity, either by themselves or in combination with 2.5 μM COL. Briefly, the assay was performed in 96-wells plates containing 20 μM of each inhibitor, diluted in DMSO, in 100 μL of MM with 10^4 conidia/mL, alone or in combination with COL. Plates were incubated at 37 °C without shaking for 48 h and the inhibition of growth was visually evaluated, and compounds with less than 20% of growth were selected for validation. As negative controls, wells with only MM and dimethyl sulfoxide (DMSO) were used. These experiments were done in duplicate. Validation was performed using alamar blue to measure the inhibition of *A. fumigatus* metabolic activity by the selected PKI by itself or in combination with COL, as previously described[36]. Briefly, 100 μL of liquid MM with 2.5×10^4 conidia/mL supplemented or not with 2.5 μM of COL plus an increasing concentration of the PKI (0 to 80 μM) and 10% of alamar blue were grown in 96-well plates for 48 h at 37 °C. Results are expressed as means ± SD from two independent experiments performed by duplicate.

Fluorescence microscopy

A total of 10^5 spores of *A. fumigatus* was inoculated on coverslips in 4 mL of MM for 16 h at 30 °C. The coverslips with adherent germlings were left untreated or treated with COL 10 μM, CAS 0.03 μg/mL, or COL 10 μM + CAS 0.03 μg/mL for different periods of time (5, 15 and 30 min). After each period, the cells were stained with propidium iodide (PI; 0.05 mg/mL; Sigma-Aldrich), and Hoechst 33342 dye (20 μg/mL; Molecular Probes, Eugene), to assess cell viability, for 5 min in the dark. In addition, an *A. fumigatus* strain with the mitochondria marked with GFP was also used to assess mitochondrial fragmentation, for which coverslips with adherent germlings were untreated or treated for 15 min. The coverslips were rinsed with PBS (140 mM NaCl, 2 mM KCl, 10 mM $NaHPO_4$, 1.8 mM KH_2PO_4, pH 7.4) and visualized on the Observer Z1 fluorescence microscope using 40x and 100x oil immersion lens objectives. Differential interference contrast (DIC) and fluorescent images were captured with an AxioCam camera (Carl Zeiss) and processed using the AxioVision software (version 4.8). Each experiment was performed twice and at least 50 germlings were counted. For PI, the wavelength excitation was 572/25 nm and emission wavelength was 629/62 nm; for Hoechst staining, the excitation wavelength was 365 nm and emission wavelength was 420–470 nm; and for GFP the wavelength excitation was 450–490 nm and emission wavelength was 500 to 550 nm.

Transcription factors (TFs), phosphatases, and kinases mutants' library screening

A total of 507 mutants from three libraries were screened to identify candidates that are sensitive to COL or COL + CAS. For the TF and phosphatase libraries 20 μM COL or 20 μM COL plus 0.2 μg/mL CAS were used. For the kinase library, 20, 40, 80 μM COL or 0.3, 0.6, and 20 μM COL plus 0.2 μg/mL CAS were used. For the primary screening, 96-wells microplates were used, where 10^4 spores/mL of each mutant was added per well in 100 μL of liquid MM without any treatment, with 20 μM of COL, 0.2 μg/mL of CAS or a combination of both drugs. After 48 h of incubation at 37 °C without agitation, growth was determined visually, and the mutants that showed less than 20% of growth were selected for validation. As the negative control, wells with only MM and DMSO were used. These experiments were done in duplicate. Validation was performed using alamar blue to measure the inhibition of the mutants' metabolic activity by the different treatments, as previously described[36]. Briefly, 100 μL of liquid MM with 2.5×10^4 conidia/mL supplemented or not with 0.2 μg/mL CAS plus an increasing concentration of COL (0 to 80 μM) and 10% of alamar blue were grown in 96-well plates for 48 h at 37 °C. Results are expressed as means ± standard deviation (SD) from two independent experiments performed by duplicate.

Radial growth

Plates containing solid MM alone, MM with different concentrations of COL (20, 40, and 80 μM), MM with different concentrations of COL (20, 40, and 80 μM) plus CAS 0.06 μg/mL, MM with different concentrations of Ca^{2+} (25, 50 and 100 mM), and MM with different concentrations of Ca^{2+} (25, 50, and 100 mM) plus 40 μM COL were centrally inoculated with 5;μL containing 10^4 spores of the different *A. fumigatus* strains. After 4 days of incubation at 37 °C, radial growth was measured. All plates were grown in triplicate in two experimental replicates and the results are expressed as means ± SD.

Statistical analyses

Graphics buildings and statistical analyses were performed using the GraphPad Prism 10. For comparisons with data from the wild-type strain or control conditions, the one tailed paired test, one-way, or two-way analysis of variance (ANOVA) analyses were performed.

Cytotoxicity assay

The cytotoxicity of ML was determined in A549 human lung epithelial cells using the XTT reduction assay. 2×10^5 cells/well were seeded in 96-well tissue plates and incubated in Dulbecco's Modified Eagle Medium (DMEM, ThermoFischer). After 24 h of incubation with 5% CO_2, the cells were treated with CAS 100 μg/mL, different concentrations of COL (20, 40, or 80 μM), or CAS 100 μg/mL+COL 20, 40 or 80 μM, and after 48 h of incubation, cell viability was assessed using the XTT assay. Briefly, 80 μL of a solution of XTT 1 mg/mL in DMEM, HEPES 1 M, and menadione 8 μg/mL were added to each well, and after 30 min, formazan formation was quantified spectrophotometrically at 450 nm using a microplate reader. Each treatment was performed in triplicate, and the results were plotted using GraphPad Prism (GraphPad Software, Inc.). A p-value <0.0001 was considered significant.

A549 human lung epithelial cells killing assays

The cell line A549 was cultured using DMEM supplemented with fetal bovine serum (FBS) 10% and penicillin-streptomycin 1% (Sigma-Aldrich) and seeded at a concentration of 1×10^6 cells/mL in 24-well plates (Corning). The cells were challenged with *A. fumigatus* at a multiplicity of infection of 1:10 and were then treated with CAS 50 μg/mL, COL 20 and 40 μM, or CAS 50 μg/mL+ COL 20 or 40 μM. We included untreated cells and cells treated with VOR 0.5 μg/mL as a control. The A549 cells were incubated for 24 h at 37 °C with CO_2 5%. After incubation, the culture media was removed, each well was washed 3 times with PBS 1×, and 1 mL of sterile cold water was added to recover and collect the cell monolayer. To assess the number of CFUs, 100 μL of the cell suspensions were plated on YAG and incubated at 37 °C for 4 days. When necessary, the cell suspensions were diluted at 1:100 or 1:1000, and 100 μL were plated. 50 μL of the inoculum adjusted to 1×10^3 cells/mL was also plated to correct the CFU count. Each treatment was performed in triplicate to calculate the CFU%, and the results were plotted using GraphPad Prism (GraphPad Software, Inc.). A p-value <0.0001 was considered significant.

HepG2 cytotoxicity

HepG2 cells were seeded at 1.25×10^5 cells/mL into 96 well plates (Starstedt) in a total volume of 100 μL of RPMI supplemented with 10% FBS. Plated cells were then grown overnight at 37 °C in the presence of 5% CO_2. Compounds, dissolved in ddH_2O or DMSO, with appropriate controls were then two-fold diluted into source plates and 100 μL of each concentration was subsequently added to cells where growth was continued for an additional 48 h. Following growth, 50 μL of a 1:4 dilution of Alamar Blue viability reagent (Invitrogen) was added to each well, and plates were incubated for an additional 3 h at 37 °C in the presence of 5% CO_2. Fluorescence measurements (535 nm excitation/595 nm emission) were performed using a Tecan Spark® multimode microplate reader to quantify cell viability. Fluorescence measurements were corrected for background from an average of medium controls across all plates and normalized relative cell viability was calculated by dividing an equal volume titration of relevant average solvent control and propagating standard deviation error. All experiments were performed in technical triplicate and biological duplicate.

Virulence analysis in *G. mellonella* model

G. mellonella larvae were purchased from Tianjin Huiyude Biotechnology Co., Ltd. After receiving the larvae, place them on a 37 °C constant-temperature incubator overnight and retrieve the larvae the following day to perform subsequent experiments. The concentration of caspofungin (CAS) was maintained at 0.4 ug/mL and the concentration of colistin (COL) is 40 uM. After mixing the certain concentration of drugs and the 1×10^8 conidia suspension in the indicated *A. fumigatus*, 10 μL liquid mixture were injected into *G. mellonella* larvae (~0.3 g for each) via the left prolegs. As a control group, the larvae were injected with phosphate buffered saline (PBS, pH 7.2-7.4). After injection, all the larvae were incubated for up to 8 days at 37 °C with humidity levels around 29–33%, and their survival rates were evaluated every 24 h. The procedure was conducted with groups of 10 larvae per treatment.

Virulence analysis in *C. elegans* model

C. elegans strain AU37 (*glp-4(bn2); sek-1(km4)*) was obtained from the Caenorhabditis Genetics Center (CGC; University of Minnesota) and was maintained and propagated at 15 °C on nematode growth media (NGM) seeded with *E. coli* (OP50), as previously described[117]. For infection assays, synchronized adult *C. elegans* were deposited on NGM agar plates seeded with 100 μL of *A. fumigatus* (Af293) spores (1.25×10^8 spores/mL) and incubated for 8 h at 25 °C. Following incubation, worms were washed off plates with ~10 mL M9 buffer, filtered twice through 30 μm cell strainers (pluriStrainer®) to separate worms from uningested conidia, and washed an additional 3X with ~10 mL M9 buffer before being resuspended in liquid NGM media supplemented with 90 μg/mL kanamycin, 200 μg/mL streptomycin, and 200 μg/mL ampicillin (to prevent any bacterial contamination). Worms (~50–75) were distributed to 48-well microplates containing dissolved compounds (200 uL final volume). Microplates were then sealed with parafilm and placed in plastic containers lined with wet paper towel to prevent evaporation. Microplates were incubated for 3 days at 25 °C with shaking (160 rpm), worm viability for each treatment was scored daily by manually examining the motility and response to stimulus of each worm under a stereomicroscope.

Reporting summary

Further information on research design is available in the Nature Portfolio Reporting Summary linked to this article.

Data availability

All the data are available as Supplementary Data and figures. Source data are provided with this paper.

References

1. Bongomin, F., Gago, S., Oladele, R. O. & Denning, D. W. Global and multi-national prevalence of fungal diseases-estimate precision. *J. Fungi* **3**, 57 (2017).
2. Brown, G. D. et al. Hidden killers: human fungal infections. *Sci. Transl. Med.* **4**, 165rv13 (2012).
3. Denning, D. W. Global incidence and mortality of severe fungal disease. *Lancet Infect. Dis.* **24**, e428–e438 (2024).
4. Gnat, S., Łagowski, D., Nowakiewicz, A. & Dyląg, M. A global view on fungal infections in humans and animals: opportunistic infections and microsporidioses. *J. Appl. Microbiol.* **131**, 2095–2113 (2021).
5. Guinea, J. et al. Pulmonary aspergillosis in patients with chronic obstructive pulmonary disease: incidence, risk factors, and outcome. *Clin. Microbiol. Infect.: Off. Publ. Eur. Soc. Clin. Microbiol. Infect. Dis.* **16**, 870–877 (2010).
6. Hope, W., Walsh, T. & Denning, D. Laboratory diagnosis of invasive aspergillosis. *Lancet Infect. Dis.* **5**, 609–622 (2005).
7. Shishodia, S. K., Tiwari, S. & Shankar, J. Resistance mechanism and proteins in *Aspergillus* species against antifungal agents. *Mycology* **10**, 151–165 (2019).
8. Burks, C., Darby, A., Gómez Londoño, L., Momany, M. & Brewer, M. T. Azole-resistant *Aspergillus fumigatus* in the environment: Identifying key reservoirs and hotspots of antifungal resistance. *PLoS Pathog.* **17**, e1009711 (2021).
9. Mellado, E. et al. A new *Aspergillus fumigatus* resistance mechanism conferring in vitro cross-resistance to azole antifungals involves a combination of cyp51A alterations. *Antimicrobial Agents Chemother.* **51**, 1897–1904 (2007).

10. Toyotome, T. et al. Emerging antifungal drug resistance in *Aspergillus fumigatus* and among other species of *Aspergillus*. *Curr. Fungal Infect. Rep.* **12**, 105–111 (2018).
11. Zhang, J. et al. A novel environmental azole resistance mutation in *Aspergillus fumigatus* and a possible role of sexual reproduction in its emergence. *mBio* **8**, e00791–17 (2017).
12. Camps, S. M. et al. Rapid induction of multiple resistance mechanisms in *Aspergillus fumigatus* during azole therapy: a case study and review of the literature. *Antimicrobial Agents Chemother.* **56**, 10–16 (2012).
13. Tashiro, M. et al. Correlation between triazole treatment history and susceptibility in clinically isolated *Aspergillus fumigatus*. *Antimicrobial Agents Chemother.* **56**, 4870–4875 (2012).
14. Hagiwara, D. et al. Whole-genome comparison of *Aspergillus fumigatus* strains serially isolated from patients with aspergillosis. *J. Clin. Microbiol.* **52**, 4202–4209 (2014).
15. van Rhijn, N. et al. *Aspergillus fumigatus* strains that evolve resistance to the agrochemical fungicide ipflufenoquin in vitro are also resistant to olorofim. *Nat. Microbiol.* **9**, 29–34 (2024).
16. Verweij, P. E. et al. The one health problem of azole resistance in *Aspergillus fumigatus*: current insights and future research agenda. *Fungal Biol. Rev.* **34**, 202–214 (2020).
17. Liu, M. et al. Cyp51A-based mechanism of azole resistance in *Aspergillus fumigatus*: illustration by a new 3D structural model of *Aspergillus* fumigatus CYP51A protein. *Med Mycol.* **54**, 400–408 (2016).
18. Jenks, J. D. & Hoenigl, M. Treatment of aspergillosis. *J. Fungi (Basel, Switz.)* **4**, 98 (2018).
19. Letscher-Bru, V. & Herbrecht, R. Caspofungin: the first representative of a new antifungal class. *J. Antimicrobial Chemother.* **51**, 513–521 (2003).
20. Satish, S. & Perlin, D. S. Echinocandin resistance in *Aspergillus fumigatus* has broad implications for membrane lipid perturbations that influence drug-target interactions. *Microbiol. Insights* **12**, 1178636119897034 (2019).
21. Lee, A. Ibrexafungerp: First Approval. *Drugs* **81**, 1445–1450 (2021).
22. Neoh, C. F., Jeong, W., Kong, D. C. & Slavin, M. A. The antifungal pipeline for invasive fungal diseases: what does the future hold? *Expert Review of Anti-Infective. Therapy* **21**, 577–594 (2023).
23. Puumala, E., Fallah, S., Robbins, N. & Cowen, L. E. Advancements and challenges in antifungal therapeutic development. *Clin. Microbiol. Rev.* **37**, e0014223 (2024).
24. Ashu, E. E. et al. Widespread amphotericin B-resistant strains of *Aspergillus fumigatus* in Hamilton, Canada. *Infect. Drug Resistance* **11**, 1549–1555 (2018).
25. Fan, Y., Korfanty, G. A. & Xu, J. Genetic analyses of amphotericin B susceptibility in *Aspergillus fumigatus*. *J. Fungi (Basel, Switz.)* **7**, 860 (2021).
26. Nosengo, N. Can you teach old drugs new tricks? *Nature* **534**, 314–316 (2016).
27. Kaul, G., Shukla, M., Dasgupta, A. & Chopra, S. Update on drug-repurposing: is it useful for tackling antimicrobial resistance? *Future Microbiol.* **14**, 829–831 (2019).
28. Dos Santos Nogueira, F. et al. Use of miltefosine to treat canine visceral leishmaniasis caused by *Leishmania infantum* in Brazil. *Parasites Vectors* **12**, 79 (2019).
29. PROFOUNDA, I. N. C. https://www.profounda.com (2024).
30. Wall, G., Herrera, N. & Lopez-Ribot, J. L. Repositionable compounds with antifungal activity against multidrug resistant Candida auris identified in the medicines for malaria venture's pathogen box. *J. Fungi (Basel, Switz.)* **5**, 92 (2019).
31. Barreto, T. L. et al. Miltefosine as an alternative strategy in the treatment of the emerging fungus *Candida auris*. *Int. J. Antimicrobial Agents* **56**, 106049 (2020).
32. Joffe, L. S. et al. The anti-helminthic compound mebendazole has multiple antifungal effects against *Cryptococcus neoformans*. *Front. Microbiol.* **8**, 535 (2017).
33. Revie, N. M. et al. Oxadiazole-containing macrocyclic peptides potentiate azole activity against pathogenic *Candida* species. *mSphere* **5**, e00256–20 (2020).
34. Iyer, K. R., Revie, N. M., Fu, C., Robbins, N. & Cowen, L. E. Treatment strategies for cryptococcal infection: challenges, advances and future outlook. *Nat. Rev. Microbiol.* **19**, 454–466 (2021).
35. Dos Reis, T. F. et al. Screening of chemical libraries for new antifungal drugs against *Aspergillus fumigatus* reveals sphingolipids are involved in the mechanism of action of miltefosine. *mBio* **12**, e0145821 (2021).
36. Dos Reis, T. F. et al. A host defense peptide mimetic, brilacidin, potentiates caspofungin antifungal activity against human pathogenic fungi. *Nat. Commun.* **14**, 2052 (2023).
37. Zhai, B. et al. Polymyxin B, in combination with fluconazole, exerts a potent fungicidal effect. *J. Antimicrobial Chemother.* **65**, 931–938 (2010).
38. Zeidler, U. et al. Synergy of the antibiotic colistin with echinocandin antifungals in *Candida* species. *J. Antimicrobial Chemother.* **68**, 1285–1296 (2013).
39. Adams, E. K., Ashcraft, D. S. & Pankey, G. A. In vitro synergistic activity of caspofungin plus polymyxin B against fluconazole-resistant *Candida glabrata*. *Am. J. Med. Sci.* **351**, 265–270 (2016).
40. Yousfi, H., Ranque, S., Rolain, J. M. & Bittar, F. In vitro polymyxin activity against clinical multidrug-resistant fungi. *Antimicrobial Resistance Infect. Control* **8**, 66 (2019).
41. Schwarz, P., Bidaud, A. L. & Dannaoui, E. In vitro synergy of isavuconazole in combination with colistin against *Candida auris*. *Sci. Rep.* **10**, 21448 (2020).
42. Bibi, M. et al. Combining colistin and fluconazole synergistically increases fungal membrane permeability and antifungal cidality. *ACS Infect. Dis.* **7**, 377–389 (2021).
43. Bidaud, A. L. et al. Colistin interacts synergistically with echinocandins against *Candida auris*. *Int. J. Antimicrobial Agents* **55**, 105901 (2020).
44. Schwarz, P. et al. In vitro synergy of isavuconazole combined with colistin against common *Candida* species. *Front. Cell. Infect. Microbiol.* **12**, 892893 (2022).
45. Schwarz, P. et al. In vitro activity of amphotericin B in combination with colistin against fungi responsible for invasive infections. *J. Fungi (Basel, Switz.)* **8**, 115 (2022).
46. MacCallum, D. M., Desbois, A. P. & Coote, P. J. Enhanced efficacy of synergistic combinations of antimicrobial peptides with caspofungin versus *Candida albicans* in insect and murine models of systemic infection. *Eur. J. Clin. Microbiol. Infect. Dis.: Off. Publ. Eur. Soc. Clin. Microbiol.* **32**, 1055–1062 (2013).
47. Grassi, G., Robles, N. R., Seravalle, G. & Fici, F. Lercanidipine in the management of hypertension: an update. *J. Pharmacol. Pharmacotherapeutics* **8**, 155–165 (2017).
48. Ivachtchenko, A. V., Ivashchenko, A. A., Shkil, D. O. & Ivashchenko, I. A. Aprotinin-drug against respiratory diseases. *Int. J. Mol. Sci.* **24**, 11173 (2023).
49. O'Toole, T. & Sharma, S. Physiology, Somatostatin. https://www.ncbi.nlm.nih.gov/books/NBK538327/ (2023).
50. Andrade, F. F., Silva, D., Rodrigues, A. & Pina-Vaz, C. Colistin update on its mechanism of action and resistance, present and future challenges. *Microorganisms* **8**, 1716 (2020).
51. El-Sayed et al. Colistin and its role in the era of antibiotic resistance: an extended review (2000-2019). *Emerg. Microbes Infect.* **9**, 868–885 (2020).
52. Ianevski, A., Giri, A. K. & Aittokallio, T. SynergyFinder 3.0: an interactive analysis and consensus interpretation of multi-drug

synergies across multiple samples. *Nucleic Acids Res.* **50**, W739–W743 (2022).
53. Rocha, E. M., Garcia-Effron, G., Park, S. & Perlin, D. S. A Ser678Pro substitution in Fks1p confers resistance to echinocandin drugs in *Aspergillus fumigatus*. *Antimicrob. Agents Chemother.* **51**, 4174–4176 (2007).
54. Luria, S. E. & Delbrück, M. Mutations of bacteria from virus sensitivity to virus resistance. *Genetics* **28**, 491–511 (1943).
55. Bottery, M. J., van Rhijn, N., Chown, H., Rhodes, J. L. & Celia-Sanchez, B. N. Elevated mutation rates in multi-azole resistant *Aspergillus fumigatus* drive rapid evolution of antifungal resistance. *Nat. Commun.* **15**, 10654 (2024).
56. Nomura, S., Horiuchi, T., Omura, S. & Hata, T. The action mechanism of cerulenin. I. effect of cerulenin on sterol and fatty acid biosynthesis in yeast. *J. Biochem.* **71**, 783–796 (1972).
57. Sutterwala, S. S. et al. De novo sphingolipid synthesis is essential for viability, but not for transport of glycosylphosphatidylinositol-anchored proteins, in African trypanosomes. *Eukaryot. Cell* **6**, 454–464 (2007).
58. Miyake, Y., Kozutsumi, Y., Nakamura, S., Fujita, T. & Kawasaki, T. Serine palmitoyltransferase is the primary target of a sphingosine-like immunosuppressant, ISP-1/myriocin. *Biochem. Biophys. Res. Commun.* **211**, 396–403 (1995).
59. Neubauer, M. et al. Mitochondrial dynamics in the pathogenic mold *Aspergillus fumigatus*: therapeutic and evolutionary implications. *Mol. Microbiol.* **98**, 930–945 (2015).
60. Ruf, D., Brantl, V. & Wagener, J. Mitochondrial fragmentation in *Aspergillus fumigatus* as early marker of granulocyte killing activity. *Front. Cell. Infect. Microbiol.* **8**, 128 (2018).
61. Shlezinger, N., Goldfinger, N. & Sharon, A. Apoptotic-like programed cell death in fungi: the benefits in filamentous species. *Front. Oncol.* **2**, 97 (2012).
62. Shlezinger, N. et al. Sterilizing immunity in the lung relies on targeting fungal apoptosis-like programmed cell death. *Sci. (N. Y., Ny.)* **357**, 1037–1041 (2017).
63. Persaud, R. et al. Clionamines stimulate autophagy, inhibit *Mycobacterium tuberculosis* survival in macrophages, and target Pik1. *Cell Chem. Biol.* **29**, 870–882.e11 (2022).
64. Iyer, K. R. et al. Identification of triazenyl indoles as inhibitors of fungal fatty acid biosynthesis with broad-spectrum activity. *Cell Chem. Biol.* **30**, 795–810.e8 (2023).
65. Simpkins, S. W. et al. Using BEAN-counter to quantify genetic interactions from multiplexed barcode sequencing experiments. *Nat. Protoc.* **14**, 415–440 (2019).
66. van Rhijn, N. et al. Functional analysis of the *Aspergillus fumigatus* kinome identifies a druggable DYRK kinase that regulates septal plugging. *Nat. Commun.* **15**, 4984 (2024).
67. Bourhill, T., Narendran, A. & Johnston, R. N. Enzastaurin: a lesson in drug development. *Crit. Rev. Oncol./Hematol.* **112**, 72–79 (2017).
68. Kobayashi, E., Nakano, H., Morimoto, M. & Tamaoki, T. Calphostin C (UCN–1028C), a novel microbial compound, is a highly potent and specific inhibitor of protein kinase C. *Biochem. Biophys. Res. Commun.* **159**, 548–553 (1989).
69. Rocha, M. C. et al. The *Aspergillus fumigatus pkcA* G579R mutant is defective in the activation of the cell wall integrity pathway but is dispensable for virulence in a neutropenic mouse infection model. *PLoS One* **10**, e0135195 (2015).
70. Rocha, M. C. et al. Aspergillus fumigatus MADS-Box transcription factor rlma is required for regulation of the cell wall integrity and virulence. G3 (*Bethesda, Md* 6, 2983–3002 (2016).
71. Zadra, I., Abt, B., Parson, W. & Haas, H. xylP promoter-based expression system and its use for antisense downregulation of the *Penicillium chrysogenum* nitrogen regulator NRE. *Appl. Environ. Microbiol.* **66**, 4810–4816 (2000).
72. Damveld, R. A. et al. The *Aspergillus niger* MADS-box transcription factor RlmA is required for cell wall reinforcement in response to cell wall stress. *Mol. Microbiol.* **58**, 305–319 (2005).
73. Furukawa, T. et al. The negative cofactor 2 complex is a key regulator of drug resistance in *Aspergillus fumigatus*. *Nat. Commun.* **11**, 427 (2020).
74. Baltussen, T. J. H. et al. The C_2H_2 transcription factor SltA is required for germination and hyphal development in *Aspergillus fumigatus*. *mSphere* **8**, e0007623 (2023).
75. Dai, M., Du, W., Lu, L. & Zhang, S. Transcription factors SltA and CrzA reversely regulate calcium homeostasis under calcium-limited conditions. *Appl. Environ. Microbiol.* **89**, e0117023 (2023).
76. Rahman, S. et al. Distinct Cohorts of *Aspergillus fumigatus* transcription factors are required for epithelial damage occurring *via* contact- or soluble effector-mediated mechanisms. *Front. Cell. Infect. Microbiol.* **12**, 907519 (2022).
77. Liu, H. et al. Determining *Aspergillus fumigatus* transcription factor expression and function during invasion of the mammalian lung. *PLoS Pathog.* **17**, e1009235 (2021).
78. Du, W. et al. The C_2H_2 transcription tactor SltA contributes to azole resistance by coregulating the expression of the drug target Erg11A and the drug efflux pump Mdr1 in *Aspergillus fumigatus*. *Antimicrobial Agents Chemother.* **65**, e01839–20 (2021).
79. Greene, V., Cao, H., Schanne, F. A. & Bartelt, D. C. Oxidative stress-induced calcium signalling in *Aspergillus nidulans*. *Cell. Signal.* **14**, 437–443 (2002).
80. Nelson, G. et al. Calcium measurement in living filamentous fungi expressing codon-optimized aequorin. *Mol. Microbiol.* **52**, 1437–1450 (2004).
81. Ries, L. N. A. et al. The *Aspergillus fumigatus* CrzA transcription factor activates chitin synthase gene expression during the caspofungin paradoxical effect. *mBio* **8**, e00705–e00717 (2017).
82. Aruanno, M., Glampedakis, E. & Lamoth, F. Echinocandins for the treatment of invasive Aspergillosis: from laboratory to bedside. *Antimicrobial Agents Chemother.* **63**, e00399–19 (2019).
83. Moreno-Velásquez, S. D., Seidel, C., Juvvadi, P. R., Steinbach, W. J. & Read, N. D. Caspofungin-mediated growth inhibition and paradoxical growth in *Aspergillus fumigatus* involve fungicidal hyphal tip lysis coupled with regenerative intrahyphal growth and dynamic changes in β-1,3-glucan synthase localization. *Antimicrobial Agents Chemother.* **61**, e00710–e00717 (2017).
84. Souza, A. C. O. et al. Loss of septation initiation network (SIN) kinases blocks tissue invasion and unlocks echinocandin cidal activity against *Aspergillus fumigatus*. *PLoS Pathog.* **17**, e1009806 (2021).
85. Calise, D. G., Park, S. C., Bok, J. W., Goldman, G. H. & Keller, N. P. An oxylipin signal confers protection against antifungal echinocandins in pathogenic aspergilli. *Nat. Commun.* **15**, 3770 (2024).
86. Walker, L. A., Lee, K. K., Munro, C. A. & Gow, N. A. Caspofungin treatment of *Aspergillus fumigatus* results in ChsG-dependent upregulation of chitin synthesis and the formation of chitin-rich microcolonies. *Antimicrobial Agents Chemother.* **59**, 5932–5941 (2015).
87. Loiko, V. & Wagener, J. The paradoxical effect of echinocandins in *Aspergillus fumigatus* relies on recovery of the β-1,3-glucan synthase Fks1. *Antimicrobial Agents Chemother.* **61**, e01690–16 (2017).
88. Robbins, N. et al. An antifungal combination matrix identifies a rich pool of adjuvant molecules that enhance drug activity against diverse fungal pathogens. *Cell Rep.* **13**, 1481–1492 (2015).
89. Melo, A. M. et al. Diphenyl diselenide and its interaction with antifungals against *Aspergillus* spp. *Med. Mycol.* **59**, myaa072 (2020).
90. Diehl, C. et al. Brilacidin, a novel antifungal agent against *Cryptococcus neoformans*. *mBio* **15**, e0103124 (2024).
91. Soriani, F. M. et al. Functional characterization of the *Aspergillus fumigatus* CRZ1 homologue, CrzA. *Mol. Microbiol.* **67**, 1274–1291 (2008).

92. Fortwendel, J. R. et al. Transcriptional regulation of chitin synthases by calcineurin controls paradoxical growth of *Aspergillus fumigatus* in response to caspofungin. *Antimicrobial Agents Chemother.* **54**, 1555–1563 (2010).
93. de Castro, P. A. et al. *Aspergillus fumigatus* calcium-responsive transcription factors regulate cell wall architecture promoting stress tolerance, virulence and caspofungin resistance. *PLoS Genet. 30* **15**, e1008551 (2019).
94. Schwarz, P., Djenontin, E. & Dannaoui, E. Colistin and isavuconazole interact synergistically in vitro against *Aspergillus nidulans* and *Aspergillus niger*. *Microorganisms* **8**, 1447 (2020).
95. Teixeira-Santos, R. et al. Unveiling the synergistic interaction between liposomal amphotericin B and colistin. *Front. Microbiol.* **7**, 1439 (2016).
96. Li, J. et al. Colistin: the re-emerging antibiotic for multidrug-resistant Gram-negative bacterial infections. *Lancet Infect. Dis.* **6**, 589–601 (2006).
97. Lima, P. G., Oliveira, J. T. A., Amaral, J. L., Freitas, C. D. T. & Souza, P. F. N. Synthetic antimicrobial peptides: characteristics, design, and potential as alternative molecules to overcome microbial resistance. *Life Sci.* **278**, 119647 (2021).
98. Veerana, M. et al. Plasma-mediated enhancement of enzyme secretion in Aspergillus oryzae. *Microb. Biotechnol.* **14**, 262–276 (2021).
99. Dos Reis, T. F., Diehl, C., Pinzan, C. F., de Castro, P. A. & Goldman, G. H. Brilacidin, a host defense peptide mimetic, potentiates ibrexafungerp antifungal activity against the human pathogenic fungus *Aspergillus fumigatus*. *Microbiol. Spectr.* **12**, e0088824 (2024).
100. Jiménez-Ortigosa, C., Perez, W. B., Angulo, D., Borroto-Esoda, K. & Perlin, D. S. De novo acquisition of resistance to SCY-078 in *Candida glabrata* involves FKS mutations that both overlap and are distinct from those conferring echinocandin resistance. *Antimicrobial Agents Chemother.* **61**, e00833–17 (2017).
101. Davis, M. R., Donnelley, M. A. & Thompson, G. R. Ibrexafungerp: a novel oral glucan synthase inhibitor. *Med Mycol.* **58**, 579–592 (2020).
102. Rocha, M. C. et al. *Aspergillus fumigatus* Hsp90 interacts with the main components of the cell wall integrity pathway and cooperates in heat shock and cell wall stress adaptation. *Cell. Microbiol.* **23**, e13273 (2021).
103. Kafer, E. Meiotic and mitotic recombination in *Aspergillus* and its chromosomal aberrations. *Adv. Genet* **19**, 33–131 (1977).
104. Priest, S. J. et al. Factors enforcing the species boundary between the human pathogens *Cryptococcus neoformans* and *Cryptococcus deneoformans*. PLoS *Genetics* **17**, e1008871 (2021).
105. Mazoyer, A. et al. flan: an R package for inference on mutation models to cite this version: HAL Id: hal-01415996 flan: An R package for inference on mutation models. **9**, 334–351 (2017).
106. Wayne P. Reference method for broth dilution. *CLSI* (2008).
107. Nødvig, C. S., Nielsen, J. B., Kogle, M. E. & Mortensen, U. H. A CRISPR- Cas9 System for Genetic Engineering of Filamentous Fungi. *PloS one* **10**, e0133085 (2015).
108. Nødvig, C. S. et al. Efficient oligo nucleotide mediated CRISPR-Cas9 gene editing in *Aspergilli*. *Fungal Genet. Biol.: FG B* **115**, 78–89 (2018).
109. Hoof, J. B., Nødvig, C. S. & Mortensen, U. H. *Genome Editing: CRISPR- Cas9. Methods Mol. Biol. (Clifton, Nj.)* **1775**, 119–132 (2018).
110. Pham, T., Xie, X. & Lin, X. An intergenic "safe haven" region in *Aspergillus fumigatus*. *Med. Mycol.* **58**, 1178–1186 (2020).
111. Furukawa, T. et al. Exploring a novel genomic safe-haven site in the human pathogenic mould Aspergillus fumigatus. *Fungal Genet Biol.* **161**, 103702 (2022).
112. Nour-Eldin, H. H., Geu-Flores, F. & Halkier, B. A. USER cloning and USER fusion: the ideal cloning techniques for small and big laboratories. *Methods Mol. Biol. (Clifton, N. J.)* **643**, 185–200 (2010).
113. Colot, H. V. et al. A high-throughput gene knockout procedure for Neurospora reveals functions for multiple transcription factors. *Proc. Natl. Acad. Sci. USA* **103**, 10352–10357 (2006).
114. Schiestl, R. H. & Gietz, R. D. High efficiency transformation of intact yeast cells using single stranded nucleic acids as a carrier. *Curr. Genet* **16**, 339–346 (1989).
115. Malavazi, I. & Goldman, G. H. Gene disruption in *Aspergillus fumigatus* using a PCR-based strategy and in vivo recombination in yeast. *Methods Mol. Biol.* **845**, 99–118 (2012).
116. Osmani, S. A., May, G. S. & Morris, R. *Aspergillus nidulans*. *J. Cell Biol.* **104**, 1495–1504 (1987).
117. Ahamefule, C. S. et al. *Caenorhabditis Elegans*-based *Aspergillus Fumigatus* infection model for evaluating pathogenicity and drug efficacy. *Front. Cell. Infect. Microbiol.* **10**, 320 (2020).

Acknowledgements

We thank the Fundação de Amparo à Pesquisa do Estado de São Paulo (FAPESP) grant numbers 2021/04977-5 (GHG) and 2022/08556-7 (LGC), the Conselho Nacional de Desenvolvimento Científico e Tecnológico (CNPq) and Fundação Coordenação de Aperfeiçoamento do Pessoal do Ensino Superior (CAPES) grant number 405934/2022-0 (The National Institute of Science and Technology INCT Funvir), and CNPq 301058/2019-9 from Brazil to GHG, the National Institutes of Health/National Institute of Allergy and Infectious Diseases from the USA, grant R01AI153356 to GHG. This work was also funded by the Joint Canada-Israel Health Research Program, jointly supported by the Azrieli Foundation, Canada's International Development Research Center, Canadian Institutes of Health Research, and the Israel Science Foundation (GHG, LEC, NO). The views expressed herein do not necessarily represent those of IDRC or its Board of Governors. LEC is also supported by the Canadian Institutes of Health Research (CIHR) Foundation grant (FDN-154288), and is a Canada Research Chair (Tier 1) in Microbial Genomics & Infectious Disease and co-Director of the CIFAR Fungal Kingdom: Threats & Opportunities program. This work was also supported by a Grant-in-Aid for Scientific Research (B) [23K23491] for CB and YY and a Grant-in-Aid for Transformative Research Areas (A) "Latent Chemical Space" [23H04882] for YY from the Ministry of Education, Culture, Sports, Science and Technology, Japan, and a Major International (Regional) Joint Research Project between China and Brazil from National Natural Science Foundation of China (Grant W2411075 to LL). We thank LifeArc (https://www.lifearc.org/) and Dr. Márcio Lourenço Rodrigues for providing the chemical libraries, and Scynexis and GlaxoSmithKline for providing ibrexafungerp, David Harold Drewry for providing the protein kinase inhibitor library and RIKEN Center for Life Science Technologies and the Support Unit for Bio-Material Analysis for sequencing. We also thank Dr. Tobias M. Hohl for providing the *A. fumigatus* h2A:mRFP strain, and Lívia Alfaya and Marcela Savoldi for the technical assistance.

Author contributions

T.F.R., X.L., L.C.G.C., P.A.C., C.F.P., J.E.M.C., I.M., M.Y., L.A.V.I., S.F., T.D. and N.R. performed most of the experiments, Y.Y., C.B., N.O., L.E.C., L.L. and G.H.G. analyzed the data and corrected the manuscript, and G.H.G. wrote the manuscript and coordinated all the work. All the authors read and edited the manuscript.

Competing interests

L.E.C. is a co-founder and shareholder in Bright Angel Therapeutics, a platform company for development of novel antifungal therapeutics. L.E.C. is a Science Advisor for Kapoose Creek, a company that harnesses the therapeutic potential of fungi. The remaining authors declare no competing interests.

Additional information

Supplementary information The online version contains supplementary material available at https://doi.org/10.1038/s41467-025-60991-z.

Correspondence and requests for materials should be addressed to Ling Lu, Thaila Fernanda dos Reis or Gustavo H. Goldman.

Peer review information *Nature Communications* thanks Ying-Lien Chen, who co-reviewed with Ching-Yu Chen, and the other, anonymous, reviewers for their contribution to the peer review of this work. A peer review file is available.